The Thesis Committee for Babak Nasouri
Certifies that this is the approved version of the following thesis:

Near Infrared Laser Propagation and Absorption Analysis in Tissues Using Forward and Inverse Monte Carlo Methods

APPROVED BY
SUPERVISING COMMITTEE:

Supervisor:

Halil Berberoglu

Yuebing Zheng

Near Infrared Laser Propagation and Absorption Analysis in Tissues Using Forward and Inverse Monte Carlo Methods

by

Babak Nasouri, B.S.

Thesis

Presented to the Faculty of the Graduate School of

The University of Texas at Austin

in Partial Fulfillment

of the Requirements

for the Degree of

Master of Science in Engineering

The University of Texas at Austin

May, 2014

Dedication

Dedicated to my parents, for their endless support and encouragement

Acknowledgements

I would like to thank Dr. Thomas Murphy for sharing his subject expertise, particularly in implementing Monte Carlo method in MATLAB. I would also like to thank Onur Taylan in Solar Energy and Biofuels Laboratory for his invaluable helps and advices through my research. I would also like to thank all of the lab members for providing me a friendly and comfortable lab environment: Akhil Kulkarni, Mahesh Venkatesan, Cody Bond, David Navar, Danniel Campbell, Joey Anthony, Daniel Pinero, Rudy Torres and Luis Galindo. Most importantly, I would like to thank my advisor, Dr. Halil Berberoglu, who has been not only a great and knowledgeable professor, but also a reliable friend that I can always look up to.

Finally, I would like to gratefully acknowledge the funding provided by LaserStim, Inc. and the fruitful discussions of Kim Segal LAT.

Near Infrared Laser Propagation and Absorption Analysis in Tissues Using Forward and Inverse Monte Carlo Methods

Babak Nasouri, M.S.E.

The University of Texas at Austin, 2014

Supervisor: Halil Berberoglu

For understanding the mechanisms of low level laser/light therapy (LLLT), accurate knowledge of light interaction with tissue is necessary. In order to have a successful therapy, laser energy needs to be delivered effectively to the target location which depending on the application can be within various layers of skin or deeper. The energy deposition is controlled by input parameters such as wavelength, beam profile and laser power, which should be selected appropriately. This thesis reports a numerical study that investigates the laser penetration through the human skin and also provides a scale for selection of wavelength, beam profile and laser power for therapeutic applications.

First, human skin is modeled as a three-layer participating medium, namely epidermis, dermis, and subcutaneous, where its geometrical and optical properties were

obtained from the literature. Both refraction and reflection are taken into account at the boundaries according to Snell's law and Fresnel relations. Then, a three dimensional multi-layer reduced-variance Monte Carlo tool was implemented to simulate the laser penetration and absorption through the skin. Local profiles of light penetration and volumetric absorption densities were simulated for uniform as well as Gaussian profile beams with different spreads at 155 mW average power over the spectral range from 1000 nm to 1900 nm. The results showed that lasers within this wavelength range could be used to effectively and safely deliver energy to specific skin layers as well as to achieve large penetration depths for treating deep tissues, without causing any skin damage. In addition, by changing the beam profile from uniform to Gaussian, the local volumetric dosage could be increased as much as three times for otherwise similar lasers.

In the second part of this thesis, a three-dimensional single-layer reduced-variance inverse Monte Carlo method was developed to find the optical properties of the skin using the experimental values of transmittance and reflectance. The results showed that both transmittance and reflectance scale well with transport optical thickness. Moreover, it was also shown that penetration depth is highly sensitive to the laser wavelength and varied within the range from 1.7 mm to 4.5 mm.

Table of Contents

List of Tables

List of Figures

Chapter 1

Introduction

1.1 BACKGROUND AND MOTIVATION FOR THE STUDY

As an effective method for improving tissue repair, pain reduction, and hair growth, Low Level Laser Therapy (LLLT) has become a progressively dominant therapy recently. In this method, lasers with the low power range from 10^0 to 10^3 mW and the wide spectral range from 300 nm to 10,600 nm are irradiated on the tissue [1]. The success of LLLT in expediting the healing rate of skin wounds has been vastly reported in the literature for both human and animal cases [1-8]. Fillipin *et al.* [2] and Rizzi *et al.* [3] reported that, using 904 nm gallium arsenide (Ga-As) laser LED with the average low power of 45 mW, considerable reduction was achieved in oxygen release and inflammatory responses of muscle, both of which are caused by trauma. Moreover, Hopkins *et al.* [4] showed that LLLT enhanced the healing speed on human forearm abrasion using laser diodes with wavelengths between 660 nm and 940 nm and power of 15 mW to 25 mW. Similarly, a noticeable increase in the rate of cell growth in the skin of both humans [5] and pigs [6] have been observed by using low-level lasers.

Despite the success of LLLT, the numbers of ineffective cases are not negligible. For example, da Rosa *et al.* [9] reported that an 808 nm As-Ga-Al laser (100 mW, 3.57 W/cm^2, 40 s) enhanced the healing process of osteoarthritis more effectively than a

660nm In-Ga-Al-P laser (100 mW, 3.57 W/cm^2, 40 s), based on the experiments on 36 male adult Wistar rats. On the other hand, Taradaj *et al.* [10] claimed that LLLT application does not improve healing of venous leg ulcers in surgically and conservatively treated patients, according to their experiments with the 810 nm Ga-Al-As laser (4 J/cm^2, 65 mW) on 83 patients. These results indicate that using LLLT in a "shot in the dark" manner cannot make this method a reliable therapy method. The dependence of laser power absorption and penetration depths on input parameters, such as wavelength, power and beam profile, should be investigated more precisely to improve the understanding of laser-tissue interaction. As an approach to resolve this issue, laser penetration through tissues was studied numerically using single-layer model for the human skin [11-19]. For example, Roeva *et al.* [17] investigated laser penetration by applying LLLT on 142 patients and also evaluating the light delivery within the tissue using Monte Carlo method. They simulated the human tissue as a single layer medium with the constant optical properties, and showed the effect of absorption and scattering coefficients on the laser penetration in skin. Moreover, Stoykova *et al.* [18] considered a single layer model for periodontal tissue and investigated the influences of tissue optical properties (anisotropy factor, tissue refraction index and etc.) on energy deposition within the medium. In another case, Parvin *et al.* [19] focused on the energy distribution in dermis using Monte Carlo simulation and studied the effect of anisotropic scattering on the density of absorbed photon. Most previous studies on LLLT considered the spectral range from 600 nm to 1000 nm due to the high penetration depths associated and availability of inexpensive laser diodes within this spectral range.

In recent years, there have been significant advancements in near infrared (NIR) laser technology making inexpensive lasers in the spectral range from 1000 nm to 1900 nm available. In addition, this underutilized wavelength range can provide advantages over the more conventional range, coupling energy more effectively to the tissue for therapeutic applications. However, achieving large enough penetration depths can be challenging and wavelength selection can significantly affect the location of treatment and the dosage of radiative energy deposited. Thus, there is a need for understanding (i) the penetration of these NIR wavelengths in different skin layers as well as (ii) the dependence of the energy deposition within the difference skin layers on control parameters such as wavelength, beam profile and laser power.

Moreover, wavelength selection in LLLT can be optimized using inverse methods for a particular therapeutic application. Use of inverse methods in extracting optical properties is widely reported in the literature [20-24]. For example, Bashkatov *et al.* [22] measured the optical properties of the human skin and mucous tissues by coupling spectrophotometer results to inverse adding-doubling method. They considered human skin as a single-layer medium and reported both absorption and scattering coefficients in the spectral range from 400 nm to 2000 nm. Moreover, Rajaram *et al.* [23] presented a lookup table-based inverse model for determining the optical properties of turbid media from steady-state diffuse reflectance in the wavelength range from 400 nm to 700 nm. More recently, Hennessy *et al.* [24] performed the inverse Monte Carlo method to generate a lookup table for extracting optical properties from tissue-simulating phantom.

Consequently, these inverse methods can be employed to enhance the LLLT results by optimizing the wavelength selection based on the desired penetration depth.

1.2 Organization of the Thesis

In the first part of the study, Chapter 2, the laser propagation at different wavelengths was compared using reduced-variance Monte Carlo method. In this section skin was modeled as three-layer participating medium with variable optical properties at different layers. Moreover, the skin damage threshold in this wavelength range was investigated and the maximum permissible exposure duration was reported based on ANSI standards.

In Chapter 3, a reduced-variance inverse Monte Carlo method was developed to extract the optical properties of the single-layer skin, based on the intended reflectance and transmittance. The implemented simulation tool was then verified using the available benchmark solutions. Finally, a lookup was generated to provide a scale for selection of wavelength in the spectral range from 1000 nm to 1900 nm.

Chapter 2

Light Propagation through the Human Skin; Forward Monte Carlo Method

This chapter presents a numerical study on laser propagation in human skin using a reduced-variance Monte Carlo method. The wavelength range from 1000 nm to 1900 nm has been considered and the energy deposition within skin layers in this spectral range is explained accordingly.

2.1 ANALYSIS

To analyze the light propagation through a human tissue, a multilayer skin model was considered and laser penetration was traced by Radiative Transport Equation (RTE). Then, the Monte Carlo method was employed to solve the RTE equation for this multilayer medium.

2.1.1 Multi-layer skin model

In this study, human skin was modeled as a three layer rectangular cuboid with the specific geometry as given in Figure 2.1. The thicknesses of epidermis, dermis and subcutaneous were 0.3 mm, 1.2 mm and 3.0 mm, respectively [25]. A collimated laser beam was incident normally on the top surface of the skin (epidermis). The laser beam diameter was obtained from VetLase Inc™ and considered to be 6.1 mm.

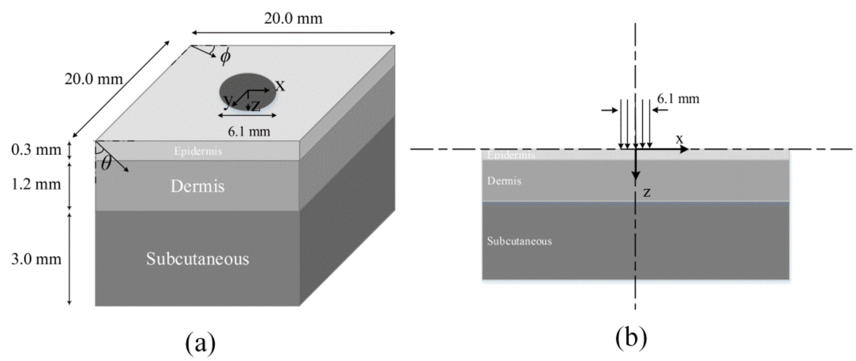

Figure 2.1: The schematic view of three layer skin model:
(a) 3-D and (b) 2-D

In order to make the problem mathematically tractable, the following assumptions were made: (1) The refractive index and asymmetry factors were constant within each layer. (2) Surrounding air had the refractive index of 1.00 and was non-participating. (3) Due to the high absorptivity of the muscle layer beneath the subcutaneous [26,27], this layer was considered radiatively cold and black. (4) The blackbody emission by skin and surrounding tissues within the wavelength range of interest was negligible at the normal body temperature of 36.5°C.

2.1.2 Governing equations and boundary conditions

Transport of laser radiation within skin can be described by the Radiative Transport Equation (RTE). The three-dimensional steady-state RTE [28] can be written as,

$$\frac{dI_\lambda(\mathrm{S},\Omega)}{dS} = -\kappa_\lambda I_\lambda(S,\Omega) - \sigma_\lambda I_\lambda(S,\Omega) + \frac{\sigma_{S,\lambda}}{4\pi}\int_{4\pi} I_\lambda(S,\Omega_i)\Phi_\lambda(\Omega_i,\Omega)d\Omega_i \tag{2.1}$$

where S is the path length, $I_\lambda(S,\Omega)$ is the local radiation intensity, κ_λ and σ_λ are the absorption and scattering coefficients of skin, respectively. Moreover, $\Phi_\lambda(\Omega_i,\Omega)$ is the scattering phase function which describes the probability of redirecting the incoming intensity from an arbitrary direction Ω_i to the direction of interest Ω . In this study, the scattering phase function is approximated with Henyey-Greenstein function [28] as,

$$\Phi_{HG}(\Omega) = \frac{1-g^2}{(1+g^2-2g\cos(\Omega))^{3/2}} \tag{2.2}$$

where, g known as the asymmetry factor, is the mean cosine of scattering angle Θ and related to the phase function by,

$$g = \overline{\cos(\Theta)} = \frac{1}{4\pi}\int_{4\pi} \Phi(\Theta)\cos(\Theta)\,\mathrm{d}\Omega_i \tag{2.3}$$

Asymmetry factor approaches +1 for strongly forward scattering media, 0 for isotropic scattering, and -1 for strongly backward scattering. In this study the asymmetry factor and the refractive index of each layer has been considered individually and are obtained from literature [29,30], over the spectral range from 1000 nm to 1900 nm. The asymmetry factors considered for epidermis, dermis and subcutaneous were 0.80, 0.91 and 0.75 and the obtained refractive indexes for these layers reported as 1.34, 1.40 and 1.44, respectively.

At the top boundary, reflectance was taken into account through the Fresnel equation according to [31],

$$\rho_\lambda = \frac{1}{2}\left[\left(\frac{n_{\lambda,1}\cos\theta_2 - n_{\lambda,2}\cos\theta_1}{n_{\lambda,1}\cos\theta_2 + n_{\lambda,2}\cos\theta_1}\right)^2 + \left(\frac{n_{\lambda,1}\cos\theta_1 - n_{\lambda,2}\cos\theta_2}{n_{\lambda,1}\cos\theta_1 + n_{\lambda,2}\cos\theta_2}\right)^2\right] \tag{2.4}$$

where θ_1 and $n_{\lambda,1}$ are the angle and the refractive index of the incident side and θ_2 and $n_{\lambda,2}$ are referred to those for the transmitted side. Here, the refraction was accounted for by Snell's law [28] as,

$$n_{\lambda,1}\sin\theta_1 = n_{\lambda,2}\sin\theta_2 \tag{2.5}$$

Finally, in the case of collimated radiation, the boundary conditions for the top surface can be written as,

$$I_\lambda(x, y, z=0) = G_{\lambda,0}\delta(\theta_c) \tag{2.6}$$

and for bottom surface,

$$I_\lambda(x, y, z=l, \pi/2 < \theta < \pi, \phi) = 0 \tag{2.7}$$

where l is the thickness of the skin and $G_{\lambda,0}$ is the incident laser irradiance which can be calculated based on the laser power used.

2.1.3 Closure laws

First, the radiation characteristics of the skin layers in the wavelength range of 1000 nm to 1900 nm were compiled from the results reported by Simpson *et al.* [27], Troy and Thennadil [29] and Iino *et al.* [32]. Figure 2.2 demonstrates the absorption and scattering coefficients of the skin layers in this wavelength range.

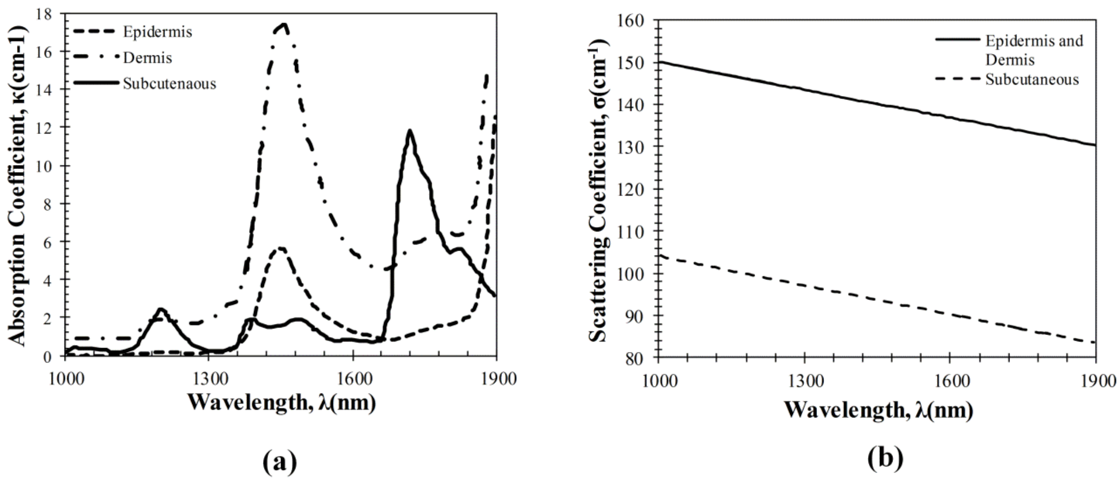

Figure 2.2: (a) Absorption and (b) scattering coefficients of human skin layers in the wavelength range from 1000 nm to 1900 nm

Then, a non-dimensional parameter, namely transport optical thickness, was used to select wavelengths of interest. Transport optical thickness indicates the overall strength of the medium in attenuating radiation at a given wavelength in the penetration direction. It can be written as,

$$\tau_\lambda = \sum_{i=1}^{n} d_i \kappa_i + \sum_{i=1}^{n} (1 - g_i) d_i \sigma_i \tag{2.8}$$

where d_i is the physical thickness, n is number of layers, g is the asymmetry factor, κ_λ and σ_λ are absorption and scattering coefficients of the i^{th} layer, respectively. Figure 2.3 illustrates this parameter for the wavelengths between 1000 nm to 1900 nm. As inadequate penetration is an issue at these larger wavelengths, wavelengths that corresponded to relatively low transport optical thicknesses have been considered, as indicated.

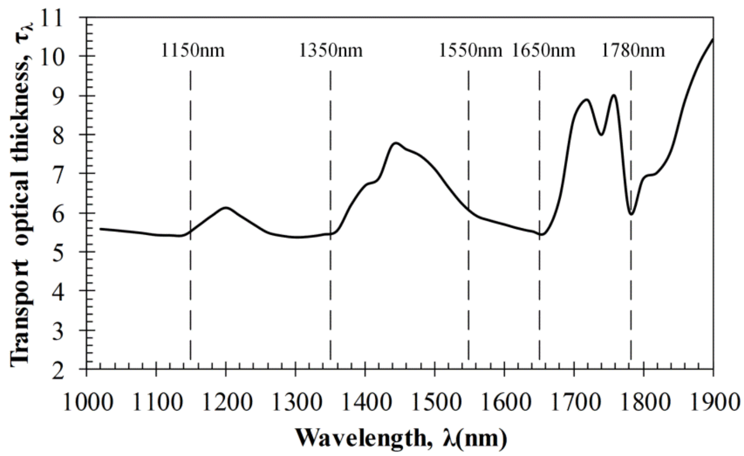

Figure 2.3: Transport optical thickness of human skin for wavelengths between 1000 nm to 1900 nm

2.1.3 Method of solution

In this study, a three-dimensional multi-layer reduced-variance Monte Carlo method was implemented and validated against benchmark solutions. The Monte Carlo technique was first proposed by Metropolis and Ulam [33] as a statistical approach for studying differential equations. More recently, Prahl *et al.* [16] applied the variance reduction technique, proposed by Kahn and Harris [34], to the Monte Carlo method and implemented a reduced-variance Monte Carlo for simulating light propagation in tissue. By using the variable step-size walking process in this method, the high variance in the normal Monte Carlo method can be resolved without a considerable CPU time increase. To illustrate, light is modeled as a large number of packets that carry a specific amount of energy (i.e., 1.0). The method tracks each energy packet as it is absorbed, scattered, back-scattered, transmitted or reflected within the skin. For the packets which scatter within the skin, a fraction of their energy will be absorbed and deducted at each interaction as,

$$W = \frac{\kappa_\lambda}{\kappa_\lambda + \sigma_\lambda} W_0 \tag{2.9}$$

where W_0 is the packet's initial energy, and W is the packet's energy after the interaction. Based on this method, a packet can propagate infinitely and its energy will never reach zero. Thus, an energy threshold is defined to terminate the packet with an energy level below the threshold. This threshold energy level was optimized to ensure that the results are independent of this selection so energy of 0.001 was considered for this study. In order to track late-stage propagation, such a weakened packet is given a second chance in m^{th} (i.e., $m = 10$) stage of surviving through roulette technique. According to this technique, if a packet was not absorbed by the ninth interaction with the medium, the roulette will either empower it to mW or eliminate it, on a random basis. The killed packets are monitored to satisfy the energy conservation. Then, based on the statistical results of the energy packets, the absorptivity and transmittance for the considered skin can be calculated. Figure 2.4 shows the flow chart for this multi-layer three-dimensional reduced-variance Monte Carlo scheme used in this study.

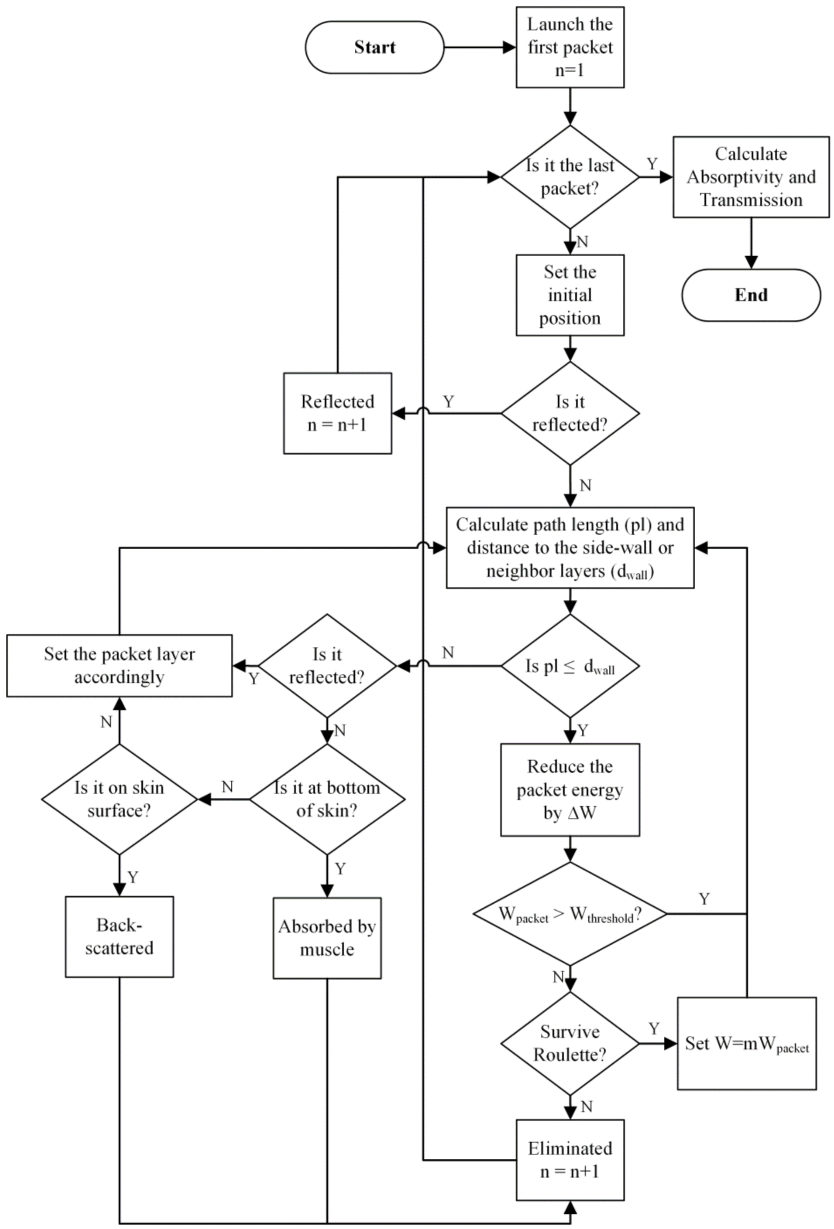

Figure 2.4: The flow chart of solution algorithm used in this study for the multi-layer three-dimensional reduced-variance Monte Carlo scheme

This code was validated for both scattering and non-scattering media cases. In the non-scattering case, a rectangular cuboid of water has been considered as a purely absorbing medium. Transmissivity of the cuboid layer was obtained from Monte Carlo method as well as Beer-Lambert's law [28], using Wieliczka *et al.* [35] data for water optical properties. In the case of anisotropic media, a medium with the optical thickness of 2.0, albedo of 0.9 and asymmetry factor of 0.75 was simulated and the obtained results were compared to those of Van de Hulst [36] and Prahl *et al.*[16]. Based on these comparisons, the percent deviations for the transmittance with respect to the Beer-Lambert law, Van de Hulst's tables and Prahl *et al.* were 0.01%, 0.11% and 0.30%, respectively.

Moreover, the sensitivity of the Monte Carlo code on the number of energy bundles used was analyzed to ensure that the obtained results were independent of this choice. By increasing the number of packets from 10^6 to 10^7, changes in the absorptance results were less than 0.1%, but the CPU time increased by 20 hours. Thus, 10^6 energy bundles with the total power of 155mW were used in all of the results reported in this chapter.

2.2 Results and Discussion

First the reduced-variance Mote Carlo simulation at the wavelength of the 1350 nm was operated to investigate the light propagation phenomena. In the next step, the simulation has been performed at the selected wavelengths to study the penetration and absorption of lasers with uniform profiles in different skin layers. Then, the results were processed in the perspective of power delivery and the selected wavelengths were compared based on this factor. Moreover, simulations for different Gaussian beam profiles were performed and dependence of laser penetration and absorption in skin on the beam profile characteristics has been shown. Lastly, the maximum allowable exposure time has been reported for the considered laser probe based on the maximum absorbed fluence and available standards.

2.2.1 Light propagation analysis at the wavelength of λ = 1350 nm

The relevant parameter in laser treatment of tissues is the dosage, i.e., the amount of energy density absorbed by tissue. Local variations of dosage can significantly affect a treatment and can be defined as,

$$D_v = P_{abs}.t_{\exp} \tag{2.10}$$

where P_{abs} is the volumetric absorbed power density (mW/mm^3) and $t_{\exp}$ is the exposure duration. Thus, here the results have been reported based on the density of absorbed power which provides the flexibility of calculating the dosage at different exposure times.

For illustrative purposes, a collimated laser beam of diameter 6.1 mm has been considered with irradiance of 155 mW at the wavelength of 1350 nm. The local absorbed power density was measured by using the results of the implemented Monte Carlo code. To do so, for a given volume, the fraction of absorbed packets were counted and multiplied to the amount of energy that each packet carries. Hence, by dividing the measured absorbed energy by its corresponding volume, the local absorbed power density was measured. Figure 2.5 shows the volumetric power density as a function of location within the three layer skin model on the $x-z$ plane. In order to generate this map, the 3D results of absorbed power within the skin were integrated in y - direction and projected on to the $x-z$ plane. Besides, in this figure, the percentages of the absorbed power at each layer are also shown. These percentages show the absorptance of laser within the skin layers so the rest of the energy packets can be either transmitted or back-scattered from the skin surface.

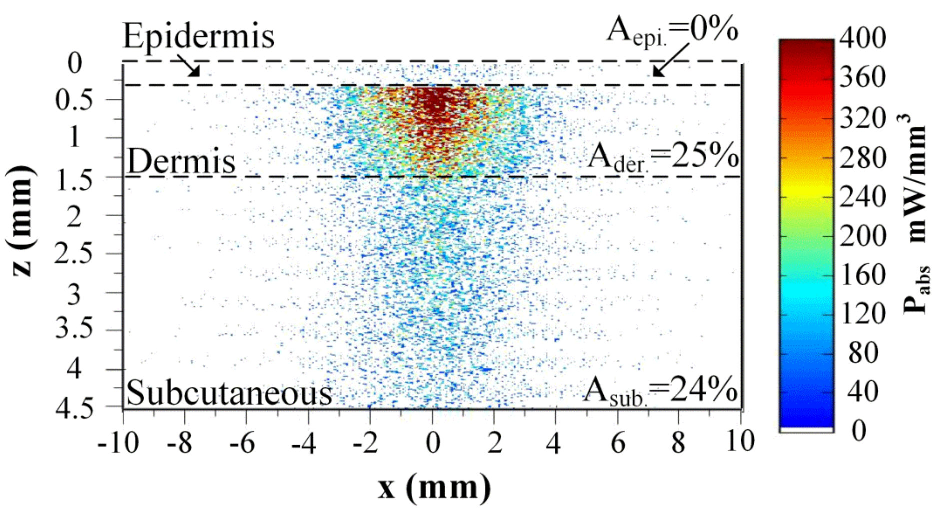

Figure 2.5: Location and volumetric density of absorbed power for P_{in}=155 mW at wavelengths of 1350 nm. Absorptance of each layer is stated in the figure in percentages; x describes the location on x; z represents the distance from the surface and colors indicate the volumetric density of absorbed power within the skin

As it can be seen in Figure 2.5, the absorbed power within the epidermis layer is negligible compared to those within dermis and subcutaneous. Moreover, although the absorptance of dermis and subcutaneous are fairly close, the propagation of the absorbed power in these two layers is different. In dermis, the dosage of absorbed power reached the highest level of 400 mW/mm^3, whereas in subcutaneous it never exceeded 200 mW/mm^3. To see the contribution of each layer to the absorption more accurately, Figure

2.6 shows the local absorbed power of skin layers as a function of distance from the skin surface. This figure shows that the local absorptance decreases for dermis and subcutaneous as the light penetrates. Based on this figure, 56% and 48% decrease in local absorptance was observed within the layers of dermis and subcutaneous, respectively. Moreover, Figure 2.6 confirms that the level of absorptance is considerably higher in dermis compared to other layers, as it was also showed in Figure 2.5.

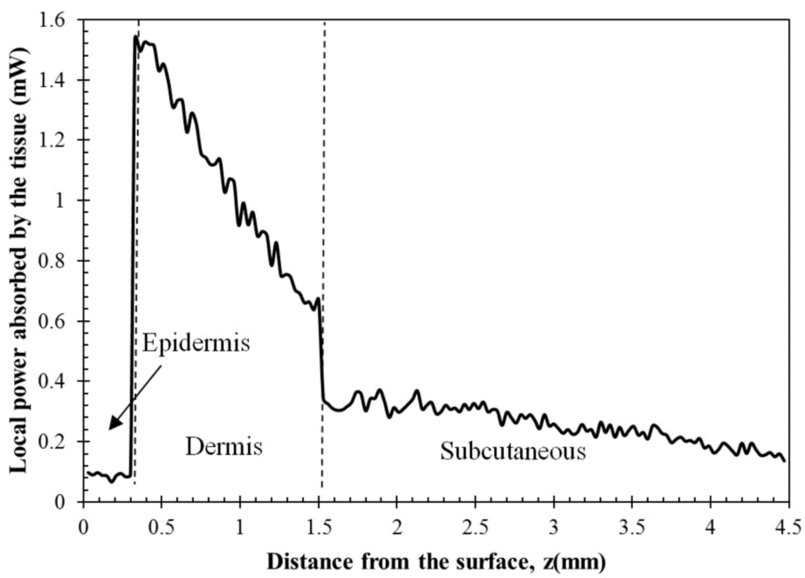

Figure 2.6: Local power absorbed within the skin as a function of distance at λ=1350 nm and P_{in} = 155 mW

2.2.2 Penetration at selected wavelengths

As it was discussed previously, in order to have the most effective result in LLLT, the laser power should be efficiently delivered to the skin layer of interest. Based on the purpose of therapy, this layer can be epidermis, dermis, subcutaneous or the muscle layer beneath the subcutaneous.

In this section, the penetration of the light at the selected wavelengths (Section 2.1.3) has been compared based on their local absorptance within their layers. To illustrate, the location of the absorbed power density within the skin has been plotted for these wavelengths in Figure 2.7. These results indicate that although the total absorptance of the skin is similar at 1150 nm, 1350 nm, and 1650 nm, the spatial distribution of absorbed power within the different layers of skin is quite different. Particularly at 1350 nm, the incident laser power is mostly delivered to the dermis, 25%, whereas in the cases of 1150 nm and 1650 nm, subcutaneous absorbed the highest percentage of the incident laser power, about 35%. Moreover, the color plots show that the distribution of absorbed power within the skin layers was highly dependent on the wavelength. For example, the volumetric power density was fairly uniform across the dermis and subcutaneous at 1150 nm whereas high volumetric absorption densities were observed in the dermis at wavelengths 1350 nm, 1550 nm, and 1650 nm. Furthermore, Figure 2.7(e) shows that unlike at any other wavelength considered, power at 1780 nm could penetrate through epidermis and dermis and get highly absorbed by subcutaneous layer. At this wavelength 90% of laser power was absorbed by subcutaneous without significant absorption in epidermis and dermis.

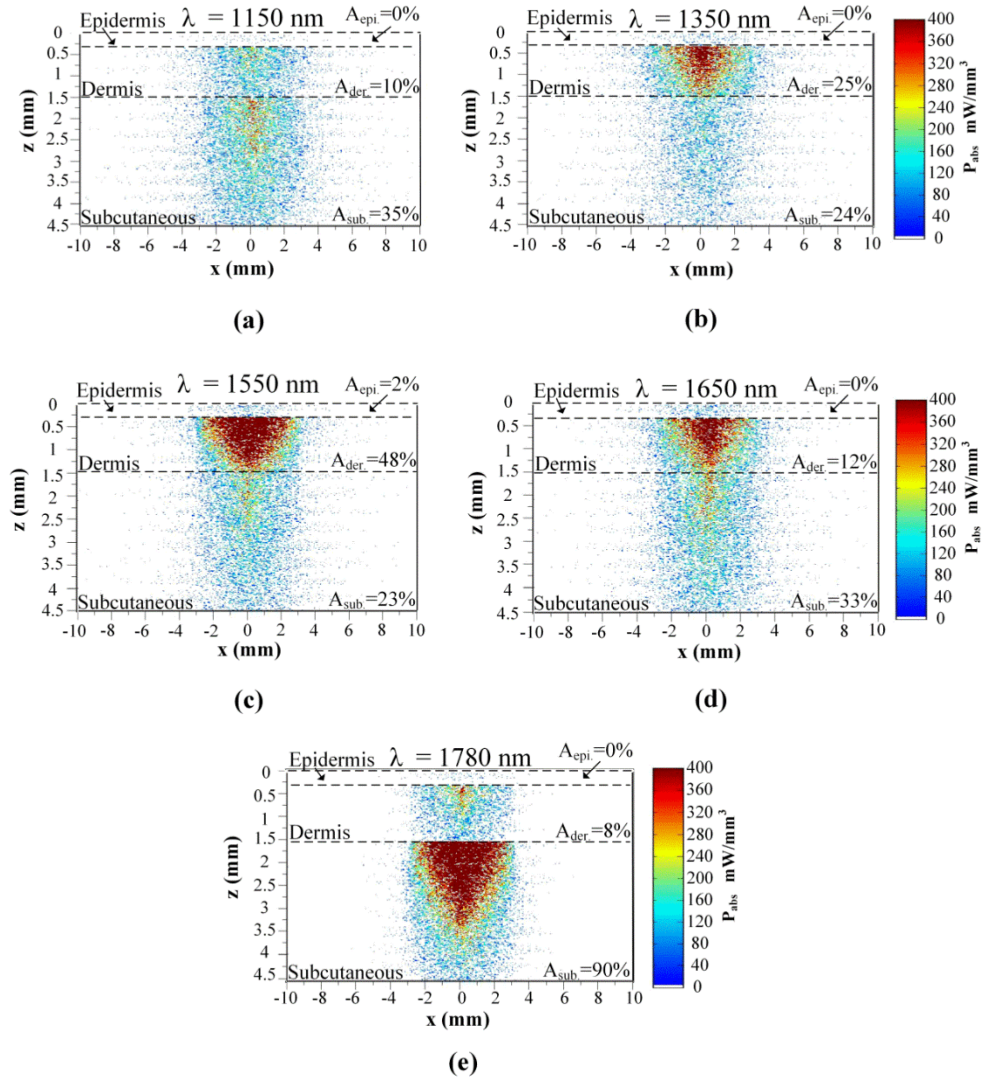

Figure 2.7: Location and volumetric density of absorbed power for P_{in}=155 mW at wavelengths of (a) 1150 nm, (b) 1350 nm, (c) 1550 nm, (d) 1650 nm and (e) 1789 nm. Absorptance of each layer is stated in the figure in percentages; x describes the location on x; z represents the distance from the surface and colors indicate the volumetric density of absorbed power within the skin

2.2.3 Dosage delivery at selected wavelengths

From the medical application perspectives, it is important to know the volume of tissue absorbing a specific dosage of energy in a given skin layer. In order to bring this point in perspective, Figure 2.8 shows the cumulative volume of skin layers, namely dermis and subcutaneous, that absorbed the power density equal to or larger than the indicated amount. To illustrate, Figure 2.8(a) demonstrates that at 1350 nm, the volume of dermis that was subjected to a power density of 250 mW/mm^3 and lower, was largest despite the fact that dermis had the largest percentage of incident power absorbed at 1550 nm. However, when the total magnitude of the highest absorptance is concerned, 1550 nm was more prevalent in delivering this range of power to dermis. In addition, Figure 2.8(a) shows that the volumetric treatment of dermis at similar power density were similar for 1150 nm with 1780 nm and 1550 nm with 1650 nm. On the other hand, Figure 2.8(b) shows that 1780 nm featured the largest power density and volume of tissue treated in subcutaneous layer. In this layer, the local power density was lower than 250 mW/ mm^3 for all other wavelengths considered where 1150 nm featured the largest volume of absorption.

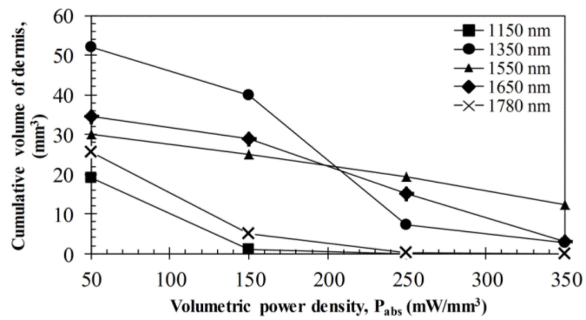

(a)

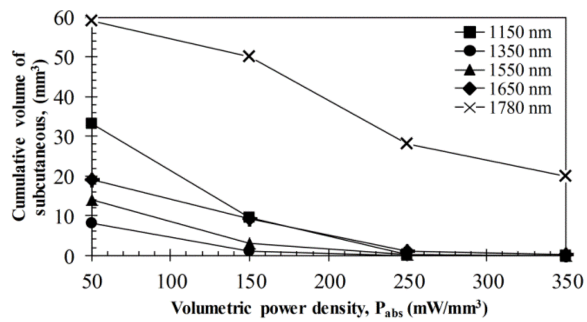

(b)

Figure 2.8: The cumulative volume of (a) dermis and (b) subcutaneous that has the power density equal to or larger than the indicated amount in the horizontal axis

In deep tissue treatments, the total power transmitted through the skin is of interest rather than the local absorptance within the different skin layers. Figure 2.9 shows the total transmitted power as a function of transport optical thickness based on the simulation results in the considered spectral range. This figure indicates that the transmitted power decreases exponentially with the transport optical thickness. Having similar transport optical thicknesses indicate that the same percentage of incident power will be transmitted through the entire skin which can be used as a first order tool for identifying and selecting wavelengths and power for deep tissue LLLT applications. As an example, at wavelength of 1650 nm, which has the transport optical thickness of 5.5, more than 41% of the laser power can be delivered to deep tissue whereas at 1250 nm, 1580 nm and 1700 nm, with the optical thicknesses of 5.6, 5.8 and 8.4, this transmitted power decreases to 37%, 29% and 1%, respectively.

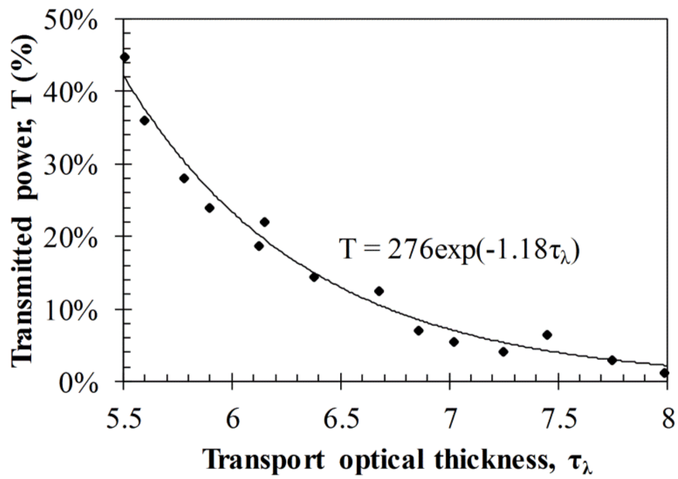

Figure 2.9: Correlation between transport optical thickness and the percentage of power than was transmitted through the entire skin without being absorbed

2.2.4 Effect of beam profile on the light propagation

For many medical laser applications, beam profile is a critical parameter. It can affect the volumetric dosage as well as the penetration depth of the incident laser power. In the previous analysis, a uniform beam profile was investigated, but a Gaussian profile is often encountered in medical applications [37]. For a laser with a Gaussian profile, the irradiance distribution is given as,

$$G_{\lambda,\mathrm{xy}} = G_{\lambda,\max} \exp\left(-\frac{x^2 + y^2}{\sigma^2}\right) \tag{2.11}$$

where $G_{\lambda,xy}$ is the local irradiance and $G_{\lambda,\max}$ is the irradiance at the beam center ($x=0, y=0$). σ is the divergence radius which indicates the specific annular distance from the center where $1/e$ of maximum irradiance has been reached. By varying this parameter the laser beam profile can be changed from a very sharp peak when $\sigma \to 0$, to the uniform profile at $\sigma \to \infty$. In order to see the influence of different spatial beam profiles on penetration and absorption, three different Gaussian beam profiles have been considered. The total power of the beams considered were the same in all cases but each feature a divergence radius of 1 mm, 2 mm and 10 mm, respectively. Figure 2.10 shows the irradiance profiles of these Gaussian beams.

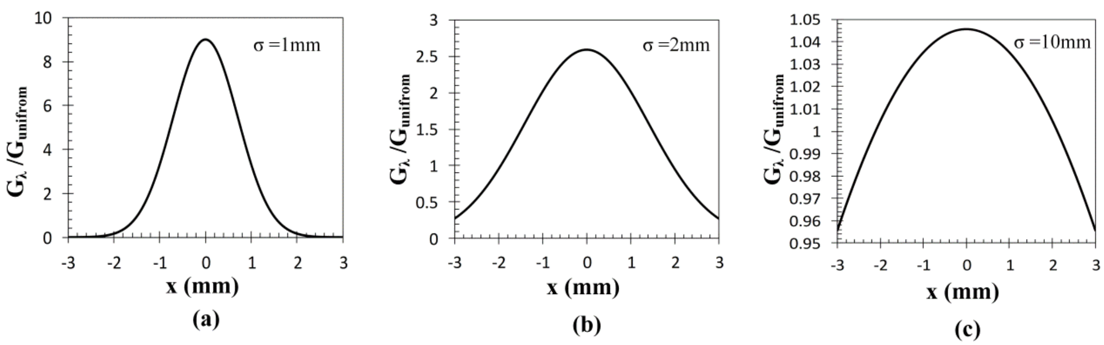

Figure 2.10: Irradiance profile of three Gaussian laser beams with a divergence radius of (a) 1mm, (b) 2mm and (c) 10mm; x is the distance from the beam center and $G_{uniform}$ is the irradiance of the uniform profile which carries the same amount of total power.

The propagation of these beams at the wavelength of 1350 nm in skin has been simulated and the results with those of the uniform profile case have been compared. Although the total absorbed and transmitted power through the entire skin was similar, there was a significant difference in the local volumetric dosages. Figure 2.11 shows the volumetric dosage for different beam profiles at the wavelength of 1350 nm. According to this figure, for the Gaussian beam with divergence radii of 10 mm, the distribution of absorbed power was similar to that of a uniform beam profile. However, smaller divergence radii results in highly localized larger volumetric dosages along the centerline of the beam.

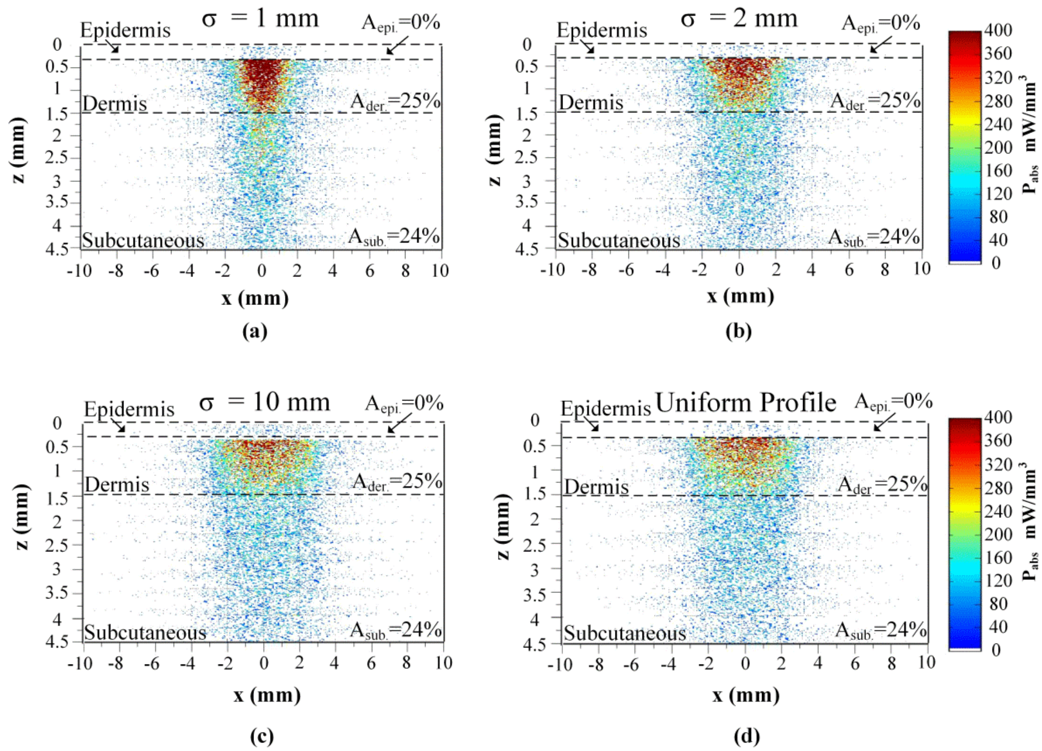

Figure 2.11: Location and volumetric dosage of absorbed energy for P_{in}=155 mW, at the wavelength of 1350 nm, for Gaussian beam profiles with divergence radii of (a) 1mm, (b) 2mm, (c) 10mm, and (d) uniform beam profile

To further illustrate this point, Figure 2.12 shows the volumetric dosage at the two different locations with respect to the beam center, namely at the beam center $x = 0$ mm and at 2 mm away from the beam center, $x = \pm 2$ mm. Figure 2.12(a) shows that by changing the beam profile from uniform to Gaussian, the dosage of absorbed power can be increased from 150 mW/mm^3 to 450 mW/mm^3 in dermis along the beam center. Similarly, in subcutaneous, the local dosage was about three times higher for the sharpest Gaussian profile in comparison to uniform beam. However, according to Figure 2.12(b), at $x = \pm\ 2$ mm, the local dosage in dermis and subcutaneous decreased from 120 mW/mm^3 to 40 mW/mm^3 and from 30 mW/mm^3 to 10 mW/mm^3, respectively.

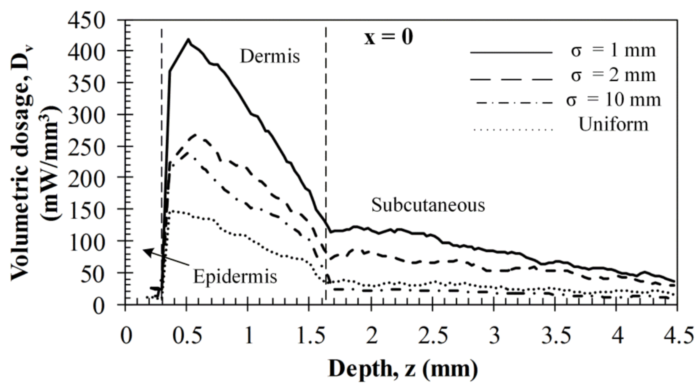

(a)

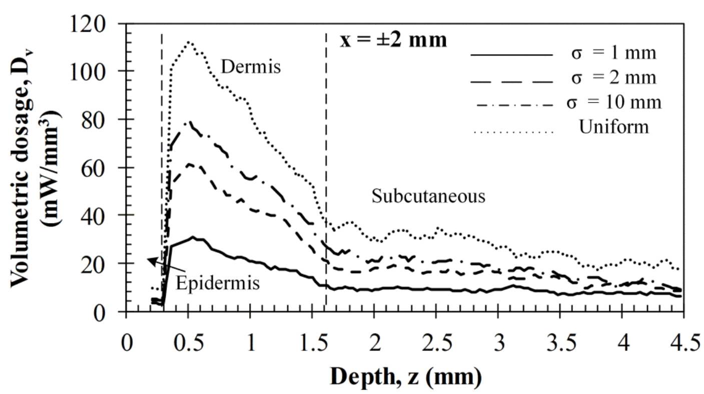

(b)

Figure 2.12: The volumetric dosage versus depth from the surface for P_{in}=155 mW, at two locations of (a) $x = 0$ and (b) $x = 2$ mm; x is the distance from the center of the beam

2.2.5 Exposure duration and skin damage threshold

Skin damage threshold can be defined as a critical amount of absorbed radiation energy, which causes permanent denaturation of skin cells. Above a critical fluence, laser irradiation causes the necrosis of tissue cells and lethal damage to superficial blood vessels [38,39]. In order to prevent this damage, the American National Standards Institute (ANSI) provides the Maximum Permissible Exposure (MPE) per area as a function of duration of exposure for different wavelengths based on experimental results [40]. These MPE data includes visible and near infrared part of the electromagnetic spectrum for wavelengths from 400 nm to 2600 nm. To find the maximum permissible exposure duration of the studied wavelengths, the maximum absorbed fluence within the skin (i.e., absorbed power per area) from the simulations was obtained and the ANSI specifications at the corresponding wavelengths were applied. Table 2.1 shows the maximum permissible exposure duration at the considered wavelengths with the laser power of p_{laser} expressed in mW. In this table the beam diameter was considered to be 6.1 mm, however, a sensitivity analysis was performed to ensure that the beam diameter does not affect the MPE values by more than 2% in the diameter range from 5 to 15 mm.

Table 2.1: Maximum permissible exposure (MPE) duration for the wavelengths of 1150, 1350, 1550, 1650 and 1780 nm at the power of p_{laser} (mW) according to ANSI Z136.1-2007 [40]

Wavelength (nm)	Permissible power range (mW)	Maximum permissible exposure duration (s)
1150	$p_{laser} \leq 10^3$	$2.9/p_{laser}$
1350	$p_{laser} \leq 10^3$	$2.3/p_{laser}$
1550	$p_{laser} \leq 700$	$10/p_{laser}$
1650	$p_{laser} \leq 700$	$10/p_{laser}$
1780	$p_{laser} \leq 700$	$10/p_{laser}$

The maximum exposure durations can easily be calculated using Table 2.1 for lasers with typical powers within the ranges of LLLT. For example, for the studied laser (i.e., 155 mW), the maximum exposure durations for the wavelength of 1150 nm and 1350 nm are about 19 s and 15 s, respectively. In addition, for higher wavelengths of 1550 nm, 1650 nm and 1780 nm, this duration can be increased up to 64 s. Although no damage in tissue is guaranteed, it should be noted that these exposure durations are on the conservative side.

2.3 CONCLUSION

In this chapter, in order to study the laser penetration through human skin, this tissue was modeled as a three-layer participating medium. A collimated laser was then incident on the top layer and penetrated through the skin. Radiative Transport Equation (RTE) was employed to simulate the laser propagation within the skin. In order to select the wavelengths of interest a dimensionless number, namely transport optical thickness, was used. Wavelengths with the lowest optical thickness were selected to maximize the penetration depth and absorbed dosage. To solve the RTE for these wavelengths, a three-dimensional multi-layer reduced-variance Monte Carlo method was implemented and validated against the benchmark solutions. This Monte Carlo method was used to evaluate the effect of wavelength and beam profile on the laser penetration through the skin. In addition, ANSI standards were employed to calculate the maximum permissible exposure duration for the considered wavelengths and laser power. Based on the results obtained, the following conclusions can be drawn:

- Based on the selected wavelength, the laser power can be efficiently delivered to the specific layer of the skin. For example, 90% absorptance in subcutaneous and 48% absorptance in dermis can be obtained by using wavelengths of 1780 nm and 1550 nm, respectively.
- Although the total absorptance at the wavelengths of 1150 nm, 1350 nm and 1650 nm are fairly close, the spatial distribution of the absorbed power within the skin layers is considerably different. To illustrate, dermis is the main absorber at the wavelength of 1350 nm, whereas in the cases of 1150 nm and 1650 nm, the incident power was mostly deposited to subcutaneous.
- Similar absorptance rate in one layer does not indicate the similar laser propagation. For example, absorptance level in dermis is fairly similar at both wavelengths of 1150 nm and 1650 nm. However, the volumetric dosage in dermis at wavelength of 1150 nm never exceeded the value of 280 mW/mm^3, while at wavelength of 1650 nm this value was as high as 400 mW/mm^3.

- In case of power delivery to dermis, wavelength of 1350 nm for dosages lower than 150 mW/mm^3 and 1550 nm for dosages higher than 250 mW/mm^3 should be utilized. In addition, wavelength of 1780 nm featured the highest power delivery to subcutaneous.
- At a given laser power, the local dosage of absorbed power can be increased about three times, by changing the beam profile from uniform (flat) to a sharp Gaussian's one.
- Maximum permissible exposure durations is inversely related to the laser power. For the laser power of 155 mW, the exposure durations can be up to 19 s and 15 s at wavelengths of 1150 nm and 1350 nm, respectively.

Chapter 3

Penetration depth correlation with optical properties; the Inverse Monte Carlo method

As discussed in Chapter 2, based on the selected wavelength, the laser power can be either absorbed within the skin layers or in muscle layer beneath the skin. For different purposes of the therapy, a particular combination of these two absorptions might be needed. For example, for deep tissue treatments the laser power is preferably deposited to the muscle layer while in hair growth, dermis is the target layer of the therapy. These two absorptions can be quantified by measuring Transmittance (T_λ), Reflectance (R_λ) and Absorption (A_λ) for a given therapy. Transmittance indicates the portion of the energy that is deposited to the muscle layer beneath the skin, absorptance stands for the portion that absorbed within the skin and reflection represents the fraction of the reflected energy. Considering that there is a negligible energy loss from sides of the medium, the following equation can be derived,

$$T_\lambda + R_\lambda + A_\lambda = 1 \tag{3.1}$$

Thus, by knowing two of these energy fractions, a therapy can be completely specified. Due to complexity of measuring the absorptance experimentally, transmittance and reflectance are mostly measured and reported through the experiments. Consequently, this chapter is focused on evaluating the light penetration based on transmittance and reflectance. First, an inverse Monte Carlo method is implemented to recover the radiation characteristics (i.e. absorption and scattering coefficient) from experimentally measured spectral transmittance and reflectance. Then, the correlation between transport optical thickness and values of transmittance and reflectance is established, using the recovered absorption and scattering coefficients. Finally, in order to investigate the effect of wavelength on penetration depth, this depth was measured and plotted in the wavelength range from 1000 nm to 1900 nm, using the forward Monte Carlo for the recovered optical properties.

3.1 ANALYSIS

To recover the absorption and scattering coefficient, a single-layer skin model was considered in this chapter. Then, an inverse Monte Carlo method was generated to retrieve these radiation characteristics from experimental values of transmittance and reflectance.

3.1.1 Single-layer skin model

Figure 3.1 shows the schematic of the skin model used in this chapter. The thickness of the skin is considered to be 4.5 mm and the laser characteristics are the same as described in Section 2.1. The collimated laser penetrates through the z-direction and propagates laterally in x-y plane.

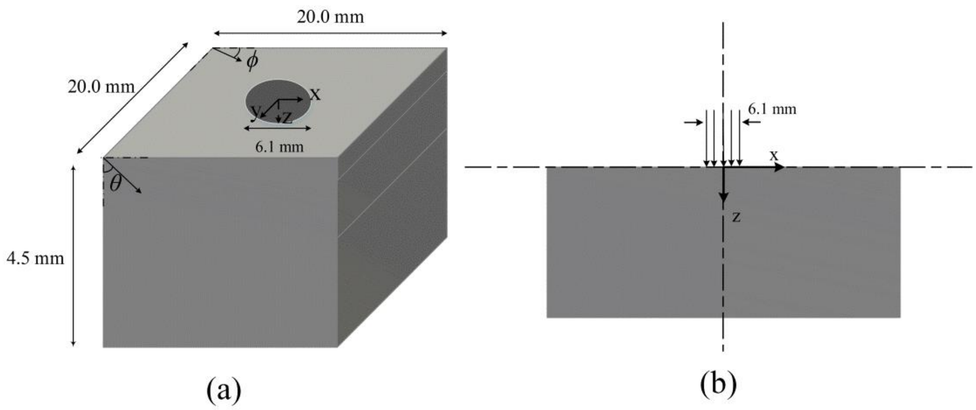

Figure 3.1: The schematic view of single-layer skin model:
(a) 3-D and (b) 2-D

In order to make the inverse problem mathematically traceable, the following assumptions were considered: (1) The refractive index and asymmetric factor are assumed to be constant within the considered wavelength range with values of 1.37 and 0.9, respectively. (2) Surrounding air had the refractive index of 1.00 and was non-participating. (3) Due to the high absorptivity of the muscle layer beneath the subcutaneous, this layer was considered radiatively cold and black [26,27]. (4) The blackbody emission by skin and surrounding tissues within the wavelength range of interest (i.e. 1000 nm to 1900 nm) was negligible at the normal body temperature of 36.5°C.

3.1.2 Method of solution

A single-layer reduced-variance inverse Monte Carlo method was implemented to find the required wavelength for obtaining the desired reflectance (R_λ) and transmittance (T_λ). In this method, for a given reflectance and transmittance, an initial set of optical properties (i.e. absorption and scattering coefficients) were assumed as the first guesses. Then, using these values, the forward Monte Carlo code (discussed in section 2.1.3) was performed to determine the reflectance and the transmittance. Next, the sum of the squared errors (e_{model}) between the predicted and intended values was calculated using,

$$e_{\text{model}} = \left[\left(\frac{R_{\text{model}} - R_{\lambda}}{R_{\lambda}} \right)^2 + \left(\frac{T_{\text{model}} - T_{\lambda}}{T_{\lambda}} \right)^2 \right]^{1/2} \tag{3.2}$$

where, R_{model} and T_{model} are the predicted values and R_λ and T_λ are the target values for reflectance and transmittance, respectively. The scattering and absorption coefficients are then iteratively updated to minimize the error using the interior point optimization method [41]. To employ this method, a reflectance-transmittance lookup table was generated. This table correlates the values of the reflectance and transmittance to their corresponding absorption and scattering coefficient within the wavelength range from 1000 nm to 1900 nm with the increments of 5 nm. Thus, a total of 180 forward Monte Carlo simulations were needed to create this lookup table. At each iteration, this lookup table was used to find the closest wavelengths ranges. Then, cubic splines were utilized to interpolate between the lookup table values and find the exact wavelength. This loop was repeated until the error, e_{model}, was lower than 5%. Figure 3.2 demonstrates the flowchart of the algorithm that used in this method.

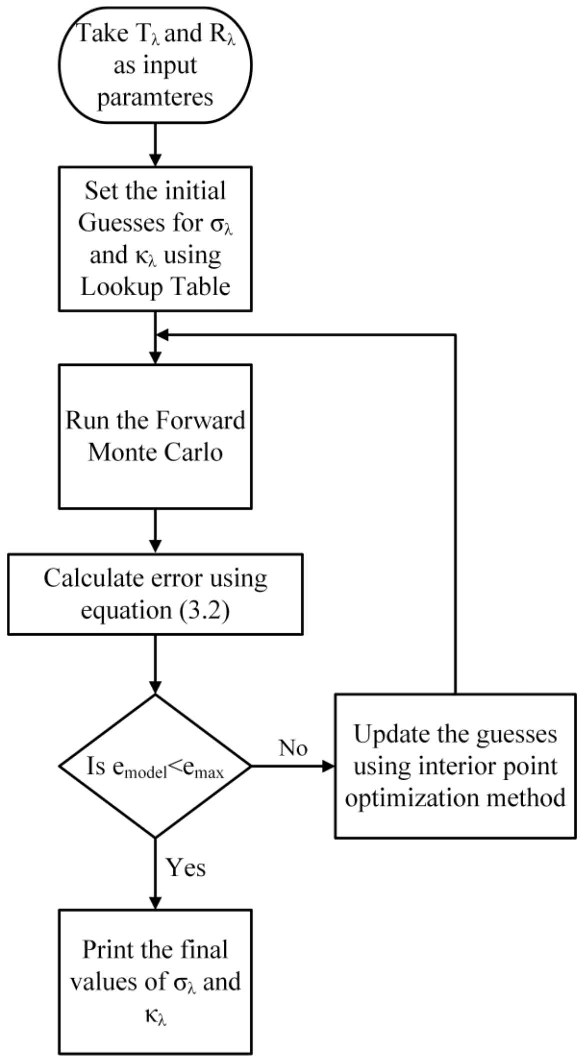

Figure 3.2: The flow chart of solution algorithm used in this study for finding the required wavelength based on given reflectance and transmittance

The forward Monte Carlo method used in this inverse problem is the single-layer version of the reduced-variance multi-layer three-dimensional Monte Carlo, described in section 2.1.3.

3.2 Results and Discussion

In this section, the accuracy and validation of the implemented inverse method is discussed first. Then, by using this verified inverse Monte Carlo tool, optical properties of the skin is recovered from the experimental values of transmittance and reflectance, obtained from literature. Finally, the correlation between transport optical thickness and experimental values of transmittance and reflectance is studied and the penetration depth of laser in LLLT is discussed as well.

3.2.1 Validation and Accuracy Analysis

To evaluate the performance of the implemented inverse Monte Carlo model, the simulation results were validated against the benchmark solutions. For a medium with the asymmetry factor of 0.75, transmittance of 66% and reflection of 0.97%, the obtained optical properties of the implemented method was verified, using the values that reported by Prahl *et al.*[17] and van de Hulst [36]. Compared to these references, the percent deviation for the absorption and scattering coefficients were measured to be 1.8% and 1.1%, respectively. In the case of isotropic scattering, the simulations results were compared to those of Giovanelli [42] and Prahl *et al.* [17] for a semi-infinite slab with total reflection of 26% and index refraction of 1.5. For this case, the percent deviation of the optical properties was lower than 2% for both scattering and absorption coefficient. Moreover, to ensure that the assumptions of constant asymmetry factor and refractive index do not affect the results considerably, a sensitivity analysis was performed. Based on this analysis, variation of the refractive index within the range of 10%, changes the values of transmittance and reflectance for no more than 1.5%. Also, a variation of 0.5% was observed by changing the asymmetry factor within the range from 0.85 to 0.95.

Furthermore, to test the accuracy of the implemented inverse Monte Carlo method, the code was utilized to determine the optical properties of the mucous membrane of the maxillary sinuses in the wavelength range from 400 nm to 2000 nm. For this simulation, the mucous membrane was modeled as a semi-infinite slab with the area of $20 \times 20\,\text{mm}^2$, asymmetry factor of 0.9 and refractive index of 1.45. Figure 3.3 compares the results of the inverse Monte Carlo method and the experimental resutls of Bashkatov *et al.* [22] for both absorption and scattering coefficients. In this figure, to better illustrate the differences between simulation results and experimental ones, reduced scattering coefficient was used instead of scattering coefficient which can be defined as,

$$\mu_s' = \sigma_\lambda (1 - g) \tag{3.3}$$

where, g is the asymmetry factor and σ_λ is the scattering coefficient of the medium. As it can be seen in this figure, the implemented method provides an excellent fit with the experimental results in both scattering and absorption coefficients. Based on these results, the inverse Monte Carlo method predicted the optical properties over the range from 400 nm to 2000 nm with the root-mean-square percent errors of 0.63% for absorption coefficient and 1.0% for reduced scattering coefficient.

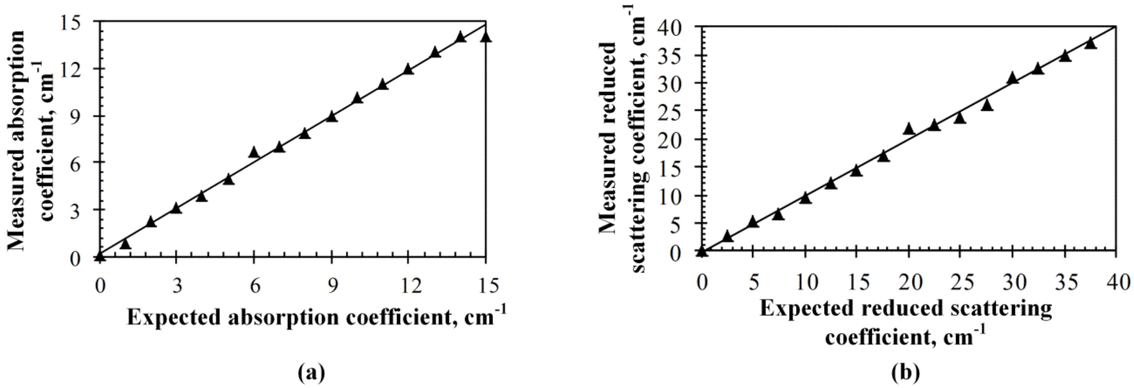

Figure 3.3: Benchmark values [22] versus simulation results for (a) absorption coefficient (b) reduced scattering coefficient of human skin in wavelength range from 400 nm to 2000 nm. The solid line indicates the perfect agreement.

Finally, since the reduced-variance Monte Carlo method was used in this inverse method, the variance of the obtained results was lower than 0.6% for all the cases. By increasing the number of energy packets from 10^6 to 10^7 the variance of the results can be decreased to about 0.1%, but the CPU time increased about 10 times for each iteration. Thus, 10^6 packets were considered for all the results reported in this chapter.

3.2.2 Retrieve of optical properties

To recover the optical properties of the skin, the experimental results of Hardy *et al.* were employed [43]. They reported the spectral values of reflectance and transmittance, using the absolute method of goniometric spectrophotometry. They obtained the excised skin samples either from surgical specimens or from autopsy and performed the experiments in the wavelength range from 600 nm to 2400 nm. Figure 3.4 shows their results for reflectance and transmittance of the human skin in the spectral range from 1000 nm to 1900 nm. This figure demonstrates that transmittance and reflectance are highly sensitive to wavelength variations. It is interesting to note that both transmittance and reflectance showed a dynamically increasing and decreasing behavior within the wavelength range from 1000 nm to 1900 nm. Moreover, the periods of these fluctuations were different for transmittance and reflectance.

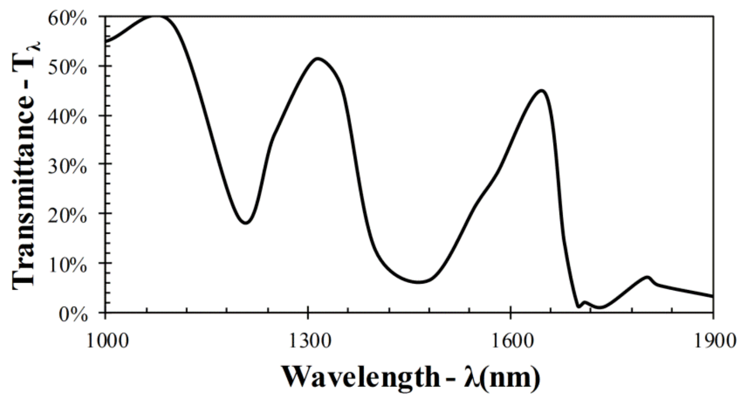

(a)

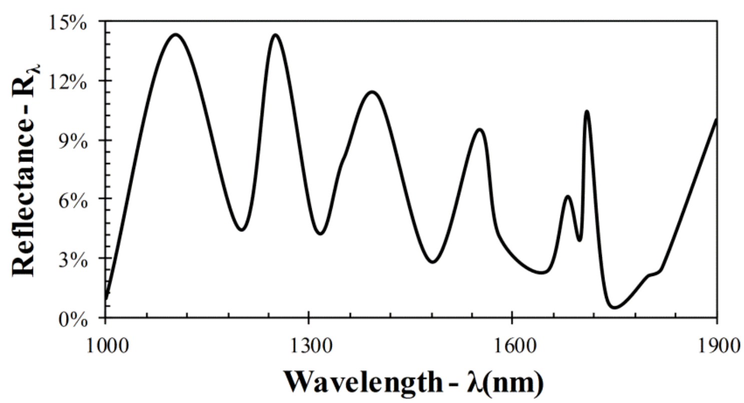

(b)

Figure 3.4: Variations of experimentally obtained (a) transmittance and (b) reflectance of human skin within the wavelength range from 1000 nm to 1900 nm [43]

In the next step, by using the experimental data given in Figure 3.4, the optical properties of the skin were obtained. Figure 3.5 shows the absorption and scattering coefficient of the human skin in this considered spectral range. To generate this figure, 60 inverse Monte Carlo simulations were performed within the range of 1000 nm to 1900 nm with the increments of 15 nm. Intermediate values were interpolated from these simulation results using the third-order polynomial interpolation.

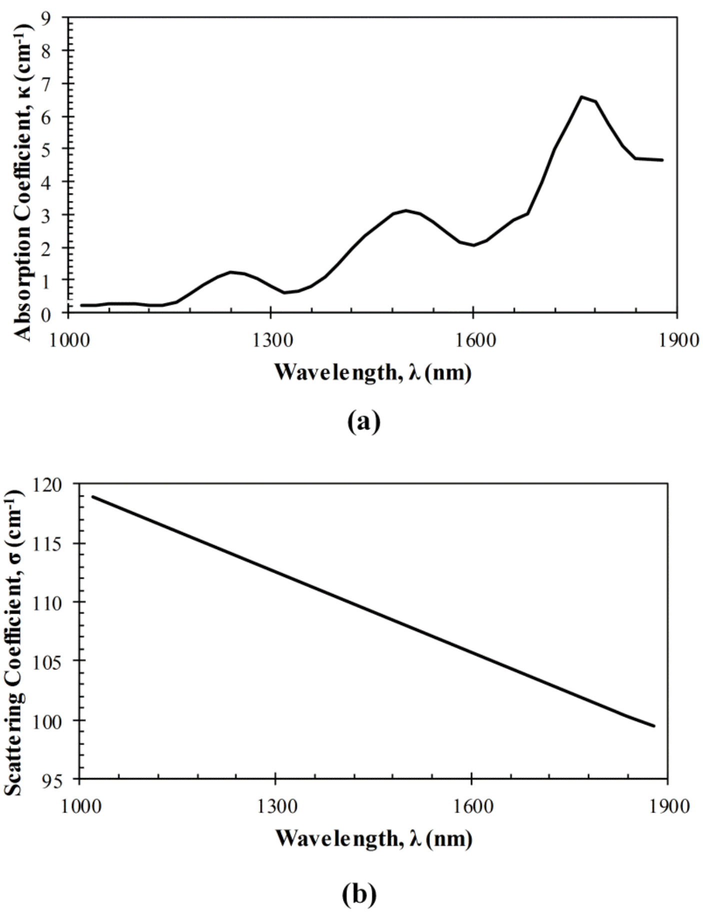

Figure 3.5: (a) Absorption and (b) scattering coefficients of human skin recovered from experimental values of transmittance and reflectance, using inverse Monte Carlo method

Then, by using the obtained absorption and scattering coefficients, the transport optical thickness can be simply measured based on Equation 2.8. To recall, transport optical thickness indicates the overall strength of the medium in attenuating radiation at a given wavelength in the penetration direction. Figure 3.6 illustrates the transmittance and reflectance as a function of transport optical thickness. According to this figure, both reflectance and transmittance decreased exponentially as the transport optical thickness increased from 5.5 to 8.0. Unlike transmittance which decreased from 45% to 3%, reflectance was less sensitive to transport optical thickness and decreased by only 7.2%. Moreover, the exponential behaviors of transmittance and reflectance confirmed that transport optical thickness can be used as a reliable tool for determining laser propagation through the skin. It means by knowing the transport optical thickness at a given wavelength, transmittance and reflectance can be calculated using the correlations given in Figure 3.6.

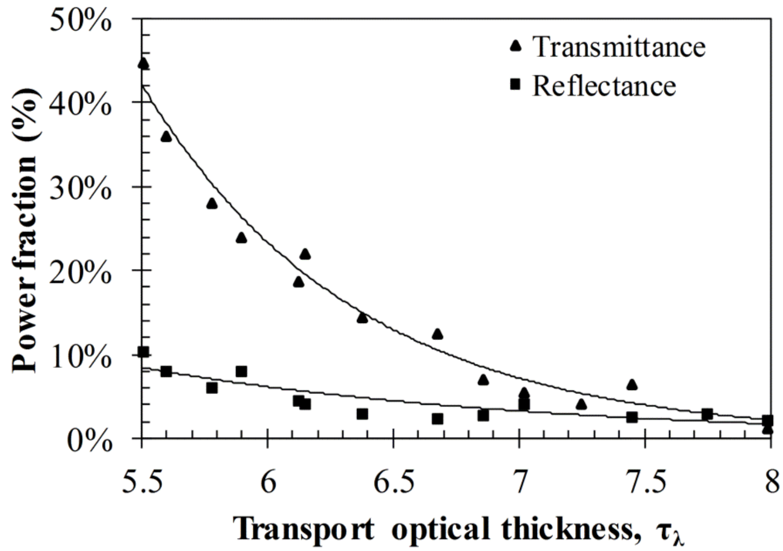

Figure 3.6: Correlation between transport optical thickness, transmittance and reflectance

Penetration depth is defined as the depth within the tissue at which the irradiance of laser falls to lower than 37% ($1/e$) of the initial irradiance. This depth indicates how deep the laser energy is deposited within the tissue. In this study, in order to calculate the penetration depth forward Monte Carlo method was performed, using the recovered optical properties. Then, based on the density of the absorbed energy at each location, penetration depth was calculated. Figure 3.7 demonstrates the penetration depth of the human skin in the wavelength range from 1000 nm to 1900 nm. Based on this figure, the penetration depth reached its lowest value at the wavelength of 1480 nm. It means at this wavelength, absorption in layers of epidermis and dermis was dominant compared to subcutaneous. Moreover, for wavelengths higher than 1700 nm, the penetration depth was between 2 mm and 2.5 mm, which confirm the fact that subcutaneous is highly absorbent at this spectral range and laser energy is mostly absorbed at the very beginning of this layer. On the other hand, in wavelength range from 1000 nm to 1450 nm, laser penetrated deeply through the human skin and the penetration depth was higher than 4.0 mm within this range. Finally, as it is shown in Figure 3.7, a wide range of penetration depths can be reached by using NIR lasers which ensures the applicability of this spectral range. Any penetration depth between 1.5 mm to 4.5 mm can be simply obtained by selecting the wavelength accordingly.

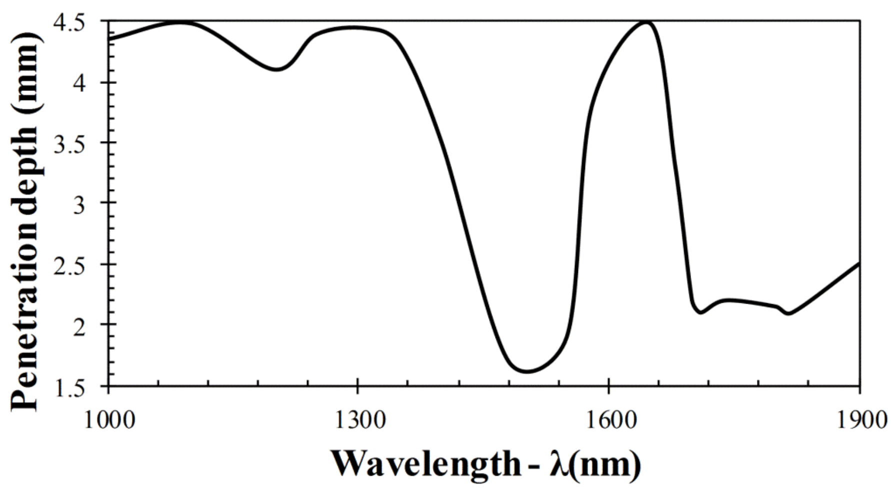

Figure 3.7: Penetration depth of laser propagation through human skin

3.2.3 Conclusion

In this chapter, a three-dimensional single-layer inverse Monte Carlo method was developed to calculate the optical properties of the skin using the experimental values of reflectance and transmittance. The implemented method was then validated against results of Prahl *et al.*, van de Hulst, Giovanelli and Bashkatov *et al.* For all these benchmark solutions the percent deviation was lower than 2%. Then, several sensitivity analyses were performed to ensure that assumption of constant asymmetry factor and refractive index does not change the output results for more than 2%. Finally, by employing the reduced-variance forward Monte code in this inverse method, uncertainties of the results were minimized to 0.6%.

In the next step, by using this validated inverse method, the optical properties of human skin were recovered from the experimental results of Hardy *et al.* It was observed that both reflectance and transmittance scale well with transport optical thickness. The exponential correlation between these factors confirmed that transport optical thickness can be utilized as a scale for comparing laser propagation through the skin. The penetration depth in this wavelength range was then calculated by performing the forward Monte Carlo code for the recovered optical properties. The major findings of this chapter can be summarized as:

- Both transmittance and reflectance showed a dynamically increasing and decreasing behavior within the wavelength range from 1000 nm to 1900 nm.
- Unlike transmittance which decreased from 45% to 3%, reflectance was less sensitive to transport optical thickness and decreased by only 7.2%.
- Transport optical thickness scales well with both transmittance and reflectance and can be used as a tool to compare the laser penetration at different wavelengths.
- At wavelengths shorter than 1450 nm, laser penetrated deeply through the skin and the penetration depth was higher than 4.0 mm.

- At wavelengths higher than 1700 nm, the penetration depths were between 2 mm and 2.5 mm, which confirm the fact that subcutaneous is highly absorbent at this range.
- The shortest penetration depth can be achieved at the wavelength of 1480 nm where this depth fell to 1.7 mm. At this wavelength, epidermis and dermis absorbed the laser energy dominantly.

Chapter 4

Conclusion and Recommendations

4.1 SUMMARY

This thesis presented numerical studies addressing the laser interaction with human skin. The study is mainly includes (i) laser propagation through the human skin using forward Monte Carlo method as well as (ii) wavelength selection analysis for medical purposes (i.e. LLLT) using inverse Monte Carlo method.

4.1.1 Light propagation through the tissue

The first part of the study provided a three-dimensional multi-layer reduced-variance Monte Carlo method for simulating the laser propagation through the human skin in the wavelength range from 1000 nm to 1900 nm. Human skin was modeled as a three layer participating medium where its properties were obtained from literature. The major findings of this part of the study can be summarized as:

- Based on the selected wavelength, the laser power can be efficiently delivered to the specific layer of the skin. For example, 90% absorptance in subcutaneous and 48% absorptance in dermis can be obtained by using wavelengths of 1780 nm and 1550 nm, respectively.
- Although the total absorptance at the wavelengths of 1150 nm, 1350 nm and 1650 nm are fairly close, the spatial distribution of the absorbed power within the skin

layers is considerably different. To illustrate, dermis is the main absorber at the wavelength of 1350 nm, whereas in the cases of 1150 nm and 1650 nm, the incident power was mostly deposited to subcutaneous.

- Similar absorptance rate in one layer does not indicate the similar laser propagation. For example, absorptance level in dermis is fairly similar at both wavelengths of 1150 nm and 1650 nm. However, the volumetric dosage in dermis at wavelength of 1150 nm never exceeded the value of 280 mW/mm^3, while at wavelength of 1650 nm this value was as high as 400 mW/mm^3.
- In case of power delivery to dermis, wavelength of 1350 nm for dosages lower than 150 mW/mm^3 and 1550 nm for dosages higher than 250 mW/mm^3 should be utilized. In addition, wavelength of 1780 nm featured the highest power delivery to subcutaneous.
- At a given laser power, the local dosage of absorbed power can be increased about three times, by changing the beam profile from uniform (flat) to a sharp Gaussian's one.
- Maximum permissible exposure durations is inversely related to the laser power. For the laser power of 155 mW, the exposure durations can be up to 19 s and 15 s at wavelengths of 1150 nm and 1350 nm, respectively.

4.1.2 Wavelength selection based on transmittance and reflectance

In the second part of the study, a reduced-variance single-layer inverse Monte Carlo method was presented to retrieve the optical properties of human skin from the experimental values of transmittance and reflectance. The inverse method was then validated against the benchmark solutions for both isotropic and anisotropic cases. In addition, several sensitivity analyses were performed to minimize the error and uncertainty of the output results. Below are the major findings of this part of study:

- Both transmittance and reflectance showed a dynamically increasing and decreasing behavior within the wavelength range from 1000 nm to 1900 nm.
- Unlike transmittance which decreased from 45% to 3%, reflectance was less sensitive to transport optical thickness and decreased by only 7.2%.
- Transport optical thickness scales well with both transmittance and reflectance and can be used as a tool to compare the laser penetration at different wavelengths.
- At wavelengths shorter than 1450 nm, laser penetrated deeply through the skin and the penetration depth was higher than 4.0 mm.
- At wavelengths higher than 1700 nm, the penetration depths were between 2 mm and 2.5 mm, which confirm the fact that subcutaneous is highly absorbent at this range.
- The shortest penetration depth can be achieved at the wavelength of 1480 nm where this depth fell to 1.7 mm. At this wavelength, epidermis and dermis absorbed the laser energy dominantly.

4.2 RECOMMENDATIONS FOR FUTURE RESEARCH

The presented thesis opens several questions to be answered through further research. Following are the recommended studies that can be performed for further understanding of the discussed subject:

- The skin model used in this study was a three layer medium with constant optical properties at each layer. However, the optical properties of skin are gradually changed through the skin layers. Thus, a more accurate skin model with variable optical properties can provide more precise results.
- The muscle layer beneath the subcutaneous was considered to be a perfect absorber due to its high value of absorption coefficient. A more accurate simulation can be performed by considering the light penetration through muscle layer and deeper as well.
- Due to excessive increase in CPU time, the number of energy packets was restricted to 10^6 bundles. Therefore, more precise results can be achieved by utilizing supercomputers.
- The implemented inverse Monte Carlo method was capable of finding the optical properties for a single-layer skin. However, skin properties are not constant through the skin layers and they change considerably as function of depth. Thus, the next step of this study can be implementing a multi-layer inverse method which would be able to measure the optical properties of each layer separately.
- Asymmetry factor as well as refractive index varies as a function of wavelength, while they were considered constant in this study. Thus, for further studies, these

two factors can be assumed as unknown values besides absorption and scattering coefficients.

- As a future research, this presented study can be coupled to the experimental set-up to obtain the optical properties of an unknown medium. Since the implemented code can be extended to the multi-layer tool, combinations of different media can be studied as well.

Appendices

Appendix A: MATLAB script for Original Monte Carlo method

Following is the main code for forward Monte Carlo method used in this study. The inputs of this code can be listed as: number of layers, slab dimensions, scattering coefficient, absorption coefficient, asymmetry factor, refractive index, phase function and number of energy packets. This code generates the location of the absorbed packets within and beneath the skin.

```
%set number of layers
n_layer=5;

% set number of packets
N_total_packets=10^6;

% set the matrix of location
loc_abs=zeros(N_total_packets,3);

% Inputs
scattering_coeff=[0,141.2,141.2,94.8,0]; %cm-1
absorption_coeff=[1000,2.7,8.58,1.69,1000];%cm-1
geometry=[4,4,2;4,4,0.03;4,4,0.12;4,4,0.3;4,4,2];%cm
ref_index=[1,1.37,1.37,1.37,1.37];
%load optical properties of layers;
load('phase_function_skin')

for i=1:n_layer
    beta(i)=scattering_coeff(i)+absorption_coeff(i);
    albedo(i)=scattering_coeff(i)./beta(i);
    length(i)=geometry(i,1);
    width(i)=geometry(i,2);
    thickness(i)=geometry(i,3);
    n(i)=ref_index(i);
end

% matrix of inputs
input=zeros(n_layer,6);
input(:,1)=beta(1,:);
input(:,2)=albedo(1,:);
input(:,3)=length(1,:);
input(:,4)=width(1,:);
input(:,5)=thickness(1,:);
input(:,6)=n(1,:);
```

```
%set number of packet hits on each wall to zero
s_abs_bottom=0;
s_packet_exit_col_top=0;
s_packet_exit_noncol_top=0;
s_missed=0;
s_abs_within=0;
for ii=1:n_layer
    str=num2str(ii);
    eval(['s_abs_within_layer_' str '=0;']) ;
end

%set the start point at layer#2
i=2;

n_count=1;
while n_count<N_total_packets

    % set initial position of packet
    radious_initial=0.306*rand;
    Angle_initial=2*pi*rand;
    x=(0.5*length(2))+radious_initial*cos(Angle_initial);
    y=(0.5*width(2))+radious_initial*sin(Angle_initial);
    z=0;
    %collimated radiation
    theta=0;
    phi=2*pi*rand;
    %run until the packet gets absotbed or exits
    packet_exit=0;
    while packet_exit==0
        packet_exit_layer=0;
        while packet_exit_layer == 0;
            if theta==0
                d_wall=thickness(i)-z;
                zhit=thickness(i);
                xhit=x;
                yhit=y;
            elseif theta==pi
                d_wall=z;
                zhit=0;
                xhit=x;
                yhit=y;
            else

[xhit,yhit,zhit,d_wall]=find_angles(x,y,z,phi,theta,length(i),
width(i),thickness(i));
            end
            path_length=(-log(rand))/beta(i);
            if path_length>d_wall
                if zhit==thickness(i) || zhit==0
                    if theta==0
```

```
                    if i==n_layer-1
                        if
rand>reflectance(theta,n(i),n(i+1))
                            s_abs_bottom=1+s_abs_bottom;
                            loc_abs(n_count,1)=xhit;
                            loc_abs(n_count,2)=yhit;

loc_abs(n_count,3)=zhit+thickness(2)+thickness(3);
                            n_count=n_count+1;
                            packet_exit=1;
                            packet_exit_layer=1;
                        else
                            x=x;
                            y=y;
                            z=thickness(i);
                            phi=phi;
                            theta=pi;
                        end
                    else
                        if
rand>reflectance(theta,n(i),n(i+1))
                            x=x;
                            y=y;
                            z=0;
                            theta=0;
                            phi=phi;
                            i=i+1;
                            packet_exit_layer=1;
                        else
                            x=x;
                            y=y;
                            z=thickness(i);
                            phi=phi;
                            theta=pi;
                        end
                    end

                elseif theta==pi
                    if i==2
                        if
rand>reflectance(theta,n(i),n(i-1))

s_packet_exit_col_top=1+s_packet_exit_col_top;
                            n_count=n_count+1;
                            packet_exit=1;
                            packet_exit_layer=1;
                        else
                            x=x;
                            y=y;
                            z=0;
                            phi=phi;
                            theta=pi;
```

```
                            end
                        else
                            if
rand>reflectance(theta,n(i),n(i-1))
                                x=x;
                                y=y;
                                z=0;
                                theta=0;
                                phi=phi;
                                i=i-1;
                                packet_exit_layer=1;
                            else
                                x=x;
                                y=y;
                                z=0;
                                phi=phi;
                                theta=pi;
                            end
                        end

                    else
                        if zhit==thickness(i)
                            if i==n_layer-1
                                if n(i)>n(i+1)
                                    if
theta>find_TIR(n(i),n(i+1));
                                        x=xhit;
                                        y=yhit;
                                        z=zhit;
                                        phi=phi;
                                        theta=pi-theta;
                                    else
                                        if
rand>reflectance(theta,n(i),n(i+1))

s_abs_bottom=s_abs_bottom+1;

loc_abs(n_count,1)=xhit;

loc_abs(n_count,2)=yhit;

loc_abs(n_count,3)=zhit+thickness(2)+thickness(3);
                                            n_count=n_count+1;
                                            packet_exit=1;

packet_exit_layer=1;
                                        else
                                            x=xhit;
                                            y=yhit;
                                            z=zhit;
                                            phi=phi;
                                            theta=pi-theta;
```

```
                                        end
                                    end
                                else
                                    if
rand>reflectance(theta,n(i),n(i+1))

s_abs_bottom=s_abs_bottom+1;

loc_abs(n_count,1)=xhit;

loc_abs(n_count,2)=yhit;

loc_abs(n_count,3)=zhit+thickness(2)+thickness(3);
                                        n_count=n_count+1;
                                        packet_exit=1;
                                        packet_exit_layer=1;
                                    else
                                        x=xhit;
                                        y=yhit;
                                        z=zhit;
                                        phi=phi;
                                        theta=pi-theta;
                                    end

                                end
                            else


                                if n(i)>n(i+1)
                                    if
theta>find_TIR(n(i),n(i+1));
                                        x=xhit;
                                        y=yhit;
                                        z=zhit;
                                        phi=phi;
                                        theta=pi-theta;
                                    else
                                        if
rand>reflectance(theta,n(i),n(i+1))
                                            x=x;
                                            y=y;
                                            z=0;
                                            phi=phi;

theta=asin((n(i)/n(i+1))*sin(theta));
                                            i=i+1;

packet_exit_layer=1;


                                        else
                                            x=xhit;
                                            y=yhit;
```

```
                                        z=zhit;
                                        phi=phi;
                                        theta=pi-theta;
                                    end
                                end
                            else
                                if rand>reflectance(theta,n(i),n(i+1))
                                    x=x;
                                    y=y;
                                    z=0;
                                    phi=phi;
                                    theta=asin((n(i)/n(i+1))*sin(theta));
                                    i=i+1;
                                    packet_exit_layer=1;
                                else
                                    x=xhit;
                                    y=yhit;
                                    z=zhit;
                                    phi=phi;
                                    theta=pi-theta;
                                end

                            end
                        end


                    elseif zhit==0
                        if i==2
                            if n(i)>n(i-1)
                                if pi-theta>find_TIR(n(i),n(i-1));
                                    x=xhit;
                                    y=yhit;
                                    z=zhit;
                                    phi=phi;
                                    theta=pi-theta;
                                else
                                    if rand>reflectance(theta,n(i),n(i-1))
                                        s_packet_exit_noncol_top=s_packet_exit_noncol_top+1;
                                        n_count=n_count+1;
                                        packet_exit=1;
                                        packet_exit_layer=1;
                                    else
                                        x=xhit;
                                        y=yhit;
                                        z=zhit;
                                        phi=phi;
```

```
                                                theta=pi-theta;
                                            end
                                        end
                                    else
                                        if
rand>reflectance(theta,n(i),n(i-1))

s_packet_exit_noncol_top=s_packet_exit_noncol_top+1;
                                            n_count=n_count+1;
                                            packet_exit=1;
                                            packet_exit_layer=1;
                                        else
                                            x=xhit;
                                            y=yhit;
                                            z=zhit;
                                            phi=phi;
                                            theta=pi-theta;
                                        end

                                    end
                                else


                                    if n(i)>n(i+1)
                                        if pi-
theta>find_TIR(n(i),n(i-1));
                                            x=xhit;
                                            y=yhit;
                                            z=zhit;
                                            phi=phi;
                                            theta=pi-theta;
                                        else
                                            if
rand>reflectance(theta,n(i),n(i-1))
                                                x=x;
                                                y=y;
                                                z=thickness(i-1);
                                                phi=phi;
                                                theta=pi-
asin((n(i)/n(i-1))*sin(pi-theta));
                                                i=i-1;

packet_exit_layer=1;
                                            else
                                                x=xhit;
                                                y=yhit;
                                                z=zhit;
                                                phi=phi;
                                                theta=pi-theta;
                                            end
                                        end
                                    else
```

```
                                    if rand>reflectance(theta,n(i),n(i-1))
                                        x=x;
                                        y=y;
                                        z=0;
                                        phi=phi;
                                        theta=pi-asin((n(i)/n(i-1))*sin(pi-theta));
                                        i=i-1;
                                        packet_exit_layer=1;
                                    else
                                        x=xhit;
                                        y=yhit;
                                        z=zhit;
                                        phi=phi;
                                        theta=pi-theta;
                                    end

                                end
                            end
                        end


                    end
                elseif xhit==0
                    s_missed=s_missed+1;
                    n_count=n_count+1;
                    packet_exit=1;
                    packet_exit_layer=1;
                elseif xhit==length(i)
                    s_missed=s_missed+1;
                    n_count=n_count+1;
                    packet_exit=1;
                    packet_exit_layer=1;
                elseif yhit==0
                    s_missed=s_missed+1;
                    n_count=n_count+1;
                    packet_exit=1;
                    packet_exit_layer=1;
                elseif yhit==width(i)
                    s_missed=s_missed+1;
                    n_count=n_count+1;
                    packet_exit=1;
                    packet_exit_layer=1;
                end
            else
                frac_traveled=path_length/d_wall;
                if theta==0
                    x=x;
                    y=y;
                    z=z+path_length;
                elseif theta==pi
```

```
                    x=x;
                    y=y;
                    z=z-path_length;
                else
                    x=x+(xhit-x)*frac_traveled;
                    y=y+(yhit-y)*frac_traveled;
                    z=z+(zhit-z)*frac_traveled;
                end
                if rand<albedo(i)
                    R_sca=rand;
                    kk=1;
                    while R_sca>=phase_function_skin(kk,7)

scattering_angle=(phase_function_skin(kk,3)+phase_function_ski
n(kk+1,3))/2;
                        kk=kk+1;
                    end
                    phi_2=2*pi*rand;
                    theta=theta+scattering_angle*cos(phi_2);
                    phi=phi+scattering_angle*sin(phi_2);
                else
                    ii=i;
                    str=num2str(ii);
                    eval(['s_abs_within_layer_' str
'=1+s_abs_within_layer_' str ';']) ;
                    loc_abs(n_count,1)=x;
                    loc_abs(n_count,2)=y;
                    if i==2
                        loc_abs(n_count,3)=z;
                    else
                        ooo=0;
                        for u=2:i-1
                            ooo=ooo+thickness(u);
                        end
                        loc_abs(n_count,3)=z+ooo;
                    end
                    s_abs_within=s_abs_within+1;
                    n_count=n_count+1;
                    packet_exit=1;
                    packet_exit_layer=1;
                end
            end
        end

    end
end

% Tally up the absorped packets(within and bottom), the missed
packets, exited from
% top(collimated and diffuese)
```

```
check_total_packets=
s_abs_bottom+s_packet_exit_col_top+s_packet_exit_noncol_top+s_
missed+s_abs_within;
absorptance=(s_abs_bottom+s_abs_within)/N_total_packets;
transmitted=s_abs_bottom/N_total_packets;
```

APPENDIX B: MATLAB SCRIPT FOR REDUCED-VARIANCE MONTE CARLO METHOD

Following is the code for reduced-variance Monte Carlo method used in this study. The inputs of this code can be listed as: number of layers, slab dimensions, scattering coefficient, absorption coefficient, asymmetry factor, refractive index, phase function, number of energy packets and threshold energy. This code generates the location of the absorbed packets within and beneath the skin.

```
clc
clear

%set number of layers,in this case the first and the last
layers are
%considered to be ambient (air)
n_layer=5;

% set number of packets
N_total_packets=10^6;

% set the matrix of location
loc_abs=zeros(N_total_packets,3);

% Inputs
absorption_coeff=[1000,1.5,6.4,6.1,1000];%cm-1
scattering_coeff=[0,132.9,132.9,85.9,0]; %cm-1
geometry=[4,4,2;4,4,0.03;4,4,0.12;4,4,0.3;4,4,2];%cm
ref_index=[1,1.34,1.4,1.44,1.44];
%load optical properties of layers;
load('phase_function_skin')

for i=1:n_layer
    beta(i)=scattering_coeff(i)+absorption_coeff(i);
    albedo(i)=scattering_coeff(i)./beta(i);
    length(i)=geometry(i,1);
    width(i)=geometry(i,2);
    thickness(i)=geometry(i,3);
    n(i)=ref_index(i);
end

% matrix of inputs
input=zeros(n_layer,6);
input(:,1)=beta(1,:);
input(:,2)=albedo(1,:);
input(:,3)=length(1,:);
input(:,4)=width(1,:);
```

```
input(:,5)=thickness(1,:);
input(:,6)=n(1,:);


%set number of packet hits on each wall to zero
w_abs_bottom=0;
w_packet_exit_col_top=0;
w_packet_exit_noncol_top=0;
w_missed=0;
w_abs_within=0;
w_threshold=0.001;

%set the start point at layer#2, considering i=1 is ambient
i=2;

n_count=1;
while n_count<N_total_packets
    while w>w_threshold && m<=10
        m=0; % Number of Interactions
        w=1; % Weight of the packets
        % set initial position of packet
        radious_initial=0.306*rand;
        Angle_initial=2*pi*rand;
        x=(0.5*length(2))+radious_initial*cos(Angle_initial);
        y=(0.5*width(2))+radious_initial*sin(Angle_initial);
        z=0;
        %collimated radiation
        theta=0;
        phi=2*pi*rand;
        %run until the packet gets absotbed or exits
        packet_exit=0;
        while packet_exit==0
            packet_exit_layer=0;
            while packet_exit_layer == 0;
                % Measuring the distance from the wall and
also the
                % potentioal hittin point
                if theta==0
                    d_wall=thickness(i)-z;
                    zhit=thickness(i);
                    xhit=x;
                    yhit=y;
                elseif theta==pi
                    d_wall=z;
                    zhit=0;
                    xhit=x;
                    yhit=y;
                else

[xhit,yhit,zhit,d_wall]=find_angles(x,y,z,phi,theta,length(i),
width(i),thickness(i));
                end
```

```
                % Calculate the path length to find out if the packet will
                % hit the wall or not
                path_length=(-log(rand))/beta(i);
                if path_length>d_wall
                    if zhit==thickness(i) || zhit==0
                        if theta==0  % If a collimated packet hits the bottom or top surface of a layer
                            if i==n_layer-1 % hitting hte last layer above ambient
                                if rand>reflectance(theta,n(i),n(i+1))
                                    w_abs_bottom=w+w_abs_bottom;
                                    loc_abs(n_count,1)=xhit;
                                    loc_abs(n_count,2)=yhit;
                                    loc_abs(n_count,3)=zhit+thickness(2)+thickness(3);
                                    m=m+1;
                                    n_count=n_count+1;
                                    packet_exit=1;
                                    packet_exit_layer=1;
                                else
                                    w_abs_bottom=w_abs_bottom+(1-albedo(i))*w;
                                    w=albedo(i)*w;
                                    m=m+1;
                                    x=x;
                                    y=y;
                                    z=thickness(i);
                                    phi=phi;
                                    theta=pi;
                                end
                            else
                                if rand>reflectance(theta,n(i),n(i+1))
                                    x=x;
                                    y=y;
                                    z=0;
                                    theta=0;
                                    phi=phi;
                                    i=i+1;
                                    packet_exit_layer=1;
                                else
                                    x=x;
                                    y=y;
                                    z=thickness(i);
                                    phi=phi;
                                    theta=pi;
```

```
w_abs_within=w_abs_within+(1-albedo(i))*w;
                                    m=m+1;
                                end
                            end

                        elseif theta==pi
                            if i==2
                                if
rand>reflectance(theta,n(i),n(i-1))

w_packet_exit_col_top=w+w_packet_exit_col_top;
                                    m=m+1;
                                    n_count=n_count+1;
                                    packet_exit=1;
                                    packet_exit_layer=1;
                                else
                                    x=x;
                                    y=y;
                                    z=0;
                                    phi=phi;
                                    theta=0;

                                end
                            else
                                if
rand>reflectance(theta,n(i),n(i-1))
                                    x=x;
                                    y=y;
                                    z=0;
                                    theta=pi;
                                    phi=phi;
                                    i=i-1;
                                    packet_exit_layer=1;
                                else
                                    x=x;
                                    y=y;
                                    z=0;
                                    phi=phi;
                                    theta=0;
                                end
                            end

                        else
                            if zhit==thickness(i)
                                if i==n_layer-1
                                    if n(i)>n(i+1)
                                        if
theta>find_TIR(n(i),n(i+1));
                                            x=xhit;
                                            y=yhit;
                                            z=zhit;
```

```
                                                    phi=phi;
                                                    theta=pi-theta;

w_abs_within=w_abs_within+(1-albedo(i))*w;
                                                    w=albedo(i)*w;
                                                    m=m+1;
                                                else
                                                    if
rand>reflectance(theta,n(i),n(i+1))

w_abs_bottom=w_abs_bottom+w;
                                                        m=m+1;

loc_abs(n_count,1)=xhit;

loc_abs(n_count,2)=yhit;

loc_abs(n_count,3)=zhit+thickness(2)+thickness(3);

n_count=n_count+1;
                                                        packet_exit=1;

packet_exit_layer=1;
                                                    else
                                                        x=xhit;
                                                        y=yhit;
                                                        z=zhit;
                                                        phi=phi;
                                                        theta=pi-
theta;

w_abs_bottom=w_abs_bottom+(1-albedo(i))*w;
                                                        w=w*albedo(i);
                                                        m=m+1;
                                                    end
                                                end
                                            else
                                                if
rand>reflectance(theta,n(i),n(i+1))

w_abs_bottom=w_abs_bottom+w;
                                                    m=m+1;

loc_abs(n_count,1)=xhit;

loc_abs(n_count,2)=yhit;

loc_abs(n_count,3)=zhit+thickness(2)+thickness(3);
                                                    n_count=n_count+1;
                                                    packet_exit=1;

packet_exit_layer=1;
                                                else
```

```
                                            x=xhit;
                                            y=yhit;
                                            z=zhit;
                                            phi=phi;
                                            theta=pi-theta;
w_abs_bottom=w_abs_bottom+(1-albedo(i))*w;
                                            w=w*albedo(i);
                                            m=m+1;
                                        end
                                    end
                                else
                                    if n(i)>n(i+1)
                                        if
theta>find_TIR(n(i),n(i+1));
                                            x=xhit;
                                            y=yhit;
                                            z=zhit;
                                            phi=phi;
                                            theta=pi-theta;
                                        else
                                            if
rand>reflectance(theta,n(i),n(i+1))
                                                x=x;
                                                y=y;
                                                z=0;
                                                phi=phi;
theta=asin((n(i)/n(i+1))*sin(theta));
                                                i=i+1;
w_abs_within=w_abs_within+(1-albedo(i))*w;
                                                w=albedo(i)*w;
                                                m=m+1;
packet_exit_layer=1;
                                            else
                                                x=xhit;
                                                y=yhit;
                                                z=zhit;
                                                phi=phi;
                                                theta=pi-
theta;
w_abs_within=w_abs_within+(1-albedo(i))*w;
                                                w=albedo(i)*w;
                                                m=m+1;
                                            end
```

```
                                        end
                                    else
                                        if rand>reflectance(theta,n(i),n(i+1))
                                            x=x;
                                            y=y;
                                            z=0;
                                            phi=phi;

                                            theta=asin((n(i)/n(i+1))*sin(theta));
                                            i=i+1;

                                            w_abs_within=w_abs_within+(1-albedo(i))*w;
                                            w=albedo(i)*w;

                                            packet_exit_layer=1;
                                        else
                                            x=xhit;
                                            y=yhit;
                                            z=zhit;
                                            phi=phi;
                                            theta=pi-theta;

                                            w_abs_within=w_abs_within+(1-albedo(i))*w;
                                            w=albedo(i)*w;
                                            m=m+1;
                                        end

                                    end
                                end

                            elseif zhit==0
                                if i==2
                                    if n(i)>n(i-1)
                                        if pi-theta>find_TIR(n(i),n(i-1));
                                            x=xhit;
                                            y=yhit;
                                            z=zhit;
                                            phi=phi;
                                            theta=pi-theta;

                                            w_abs_within=w_abs_within+(1-albedo(i))*w;
                                            w=albedo(i)*w;
                                            m=m+1;
                                        else
                                            if rand>reflectance(theta,n(i),n(i-1))

                                                w_packet_exit_noncol_top=w_packet_exit_noncol_top+w;
                                                m=m+1;
```

```
n_count=n_count+1;
                                                packet_exit=1;

packet_exit_layer=1;
                                            else
                                                x=xhit;
                                                y=yhit;
                                                z=zhit;
                                                phi=phi;
                                                theta=pi-
theta;

w_abs_within=w_abs_within+(1-albedo(i))*w;
                                                w=albedo(i)*w;
                                                m=m+1;
                                            end
                                        end
                                    else
                                        if
rand>reflectance(theta,n(i),n(i-1))

w_packet_exit_noncol_top=w_packet_exit_noncol_top+1;
                                            m=m+1;
                                            n_count=n_count+1;
                                            packet_exit=1;

packet_exit_layer=1;
                                        else
                                            x=xhit;
                                            y=yhit;
                                            z=zhit;
                                            phi=phi;
                                            theta=pi-theta;

w_abs_within=w_abs_within+(1-albedo(i))*w;
                                            w=albedo(i)*w;
                                            m=m+1;
                                        end

                                    end
                                else

                                    if n(i)>n(i+1)
                                        if pi-
theta>find_TIR(n(i),n(i-1));
                                            x=xhit;
                                            y=yhit;
                                            z=zhit;
                                            phi=phi;
                                            theta=pi-theta;
```

```
                        w_abs_within=w_abs_within+(1-albedo(i))*w;
                        w=albedo(i)*w;
                        m=m+1;
                    else
                        if rand>reflectance(theta,n(i),n(i-1))
                            x=x;
                            y=y;
                            z=thickness(i-1);
                            phi=phi;
                            theta=pi-asin((n(i)/n(i-1))*sin(pi-theta));
                            w_abs_within=w_abs_within+(1-albedo(i))*w;
                            w=albedo(i)*w;
                            m=m+1;
                            i=i-1;
                            packet_exit_layer=1;
                        else
                            x=xhit;
                            y=yhit;
                            z=zhit;
                            phi=phi;
                            theta=pi-theta;
                            w_abs_within=w_abs_within+(1-albedo(i))*w;
                            w=albedo(i)*w;
                            m=m+1;
                        end
                    end
                else
                    if rand>reflectance(theta,n(i),n(i-1))
                        x=x;
                        y=y;
                        z=0;
                        phi=phi;
                        theta=pi-asin((n(i)/n(i-1))*sin(pi-theta));
                        w_abs_within=w_abs_within+(1-albedo(i))*w;
                        w=albedo(i)*w;
                        m=m+1;
                        i=i-1;
                        packet_exit_layer=1;
                    else
                        x=xhit;
                        y=yhit;
```

```
                                                z=zhit;
                                                phi=phi;
                                                theta=pi-theta;

w_abs_within=w_abs_within+(1-albedo(i))*w;
                                                w=albedo(i)*w;
                                                m=m+1;
                                            end

                                        end
                                    end
                                end


                            end
                        elseif xhit==0
                            w_missed=w_missed+1;
                            n_count=n_count+1;
                            packet_exit=1;
                            packet_exit_layer=1;
                        elseif xhit==length(i)
                            w_missed=w_missed+1;
                            n_count=n_count+1;
                            packet_exit=1;
                            packet_exit_layer=1;
                        elseif yhit==0
                            w_missed=w_missed+1;
                            n_count=n_count+1;
                            packet_exit=1;
                            packet_exit_layer=1;
                        elseif yhit==width(i)
                            w_missed=w_missed+1;
                            n_count=n_count+1;
                            packet_exit=1;
                            packet_exit_layer=1;
                        end
                    else
                        frac_traveled=path_length/d_wall;
                        if theta==0
                            x=x;
                            y=y;
                            z=z+path_length;
                        elseif theta==pi
                            x=x;
                            y=y;
                            z=z-path_length;
                        else
                            x=x+(xhit-x)*frac_traveled;
                            y=y+(yhit-y)*frac_traveled;
                            z=z+(zhit-z)*frac_traveled;
                        end

```

```
                    R_sca=rand;
                    kk=1;
                    while R_sca>=phase_function_skin(kk,7*(i-
1))

scattering_angle=(phase_function_skin(kk,(3+7*(i-
2)))+phase_function_skin(kk+1,(3+7*(i-2))))/2;
                        kk=kk+1;
                    end
                    phi_2=2*pi*rand;
                    theta=theta+scattering_angle*cos(phi_2);
                    phi=phi+scattering_angle*sin(phi_2);
                    w_abs_within=w_abs_within+(1-albedo(i))*w;
                    w=albedo(i)*w;
                    m=m+1;

                end
            end

        end
    end
[w,m]=russian_ruolette(w);
end

% Tally up the absorped packets(within and bottom), the missed
packets, exited from
% top(collimated and diffuese)
check_total_packets=
w_abs_bottom+w_packet_exit_col_top+s_packet_exit_noncol_top+w_
missed+s_abs_within;
absorptance=(w_abs_bottom+s_abs_within)/N_total_packets;
transmitted=w_abs_bottom/N_total_packets;
```

Appendix C: MATLAB script for Inverse Monte Carlo method

Following is the code for recovering the optical properties of human skin. The inputs of this code can be listed as: Transmittance and Reflectance.

```
clear
clc
% Input Parameters
T_input=0.4;
R_input=0.05;
emax=0.05;
% Set the initial guesses using Lookup Table
[kappa,sigma]= look_up_table(T,R);

while e<=emax
[T,R]=Monte_Carlo_One_Layer(kappa,sigma);
e=((((T-T_input)/T)^2 + ((R-R_input)/R)^2)^0.5);
[T,R]= interior_update(T,R,e);
end
T_final=T;
R_final=R;
```

Bibliography

1. Y.-Y. Huang, A. C.-H. Chen, J. D. Carroll and M. R. Hamblin, “Biphasic Dose Response in Low Level Light Therapy,” *Dose-Response* **7**, 358-383 (2009).
2. L. I. Fillipin, J. L. Mauriz, K. Vendovelli, A. J. Moreira, C. G. Zettler, O. Lech, N. P. Marroni and J. Gonzalez-Gallego, “Low-Level Laser Therapy (LLLT) Prevents Oxidative Stress and Reduces Fibrosis in Rat Traumatized Achilles Tendon,” *Laser. Surg. Med.* **37**, 293-300 (2005).
3. C. F. Rizzi, J. L. Mauriz, D. S. Freitas Correa, A. J. Moreira, C. G. Zettler, L. I. Filippin, N. P. Marroni and J. Gonzalez-Gallego, “Effects of Low-Level Laser Therapy (LLLT) on the Nuclear Factor (NF)-kB Signaling Pathway in Traumatized Muscle,” *Laser. Surg. Med.* **38**, 704-713 (2006).
4. J. T. Hopkins, T. A. McLoda, J. G. Seegmiller and G. D. Baxter, “Low-Level Laser Therapy Facilitates Superficial Wound Healing in Humans: A Triple-Blind, Sham-Controlled Study,” *J. Athl. Training* **39**, 223-229 (2004).
5. L. Almeida-Lopez, J. Rigau, R. A. Zangaro, J. Guidugli-Neto and M. M. Marques Haeger, “Comparison of the Low Level Laser Therapy Effects on Cultured Human Gingival Fibroblasts Proliferation Using Different Irradiance and Same Fluence,” *Laser. Surg. Med.* **29**, 179-184 (2001).
6. R. P. Abergel, E. Glassberg and J. Uitto, “Increased Wound-Healing Rate In Pig Skin Treated By Helium-Neon Laser,” in Photoelectron Spectroscopy, M. W. Bern, Ed., *Proc. SPIE* **0908***,* 6-11 (1988).

7. J. M. Bjordal, M. I. Johnson, V. Iversen, F. Aimbire and R. A. B. Lopes-Matins, "Low-Level Laser Therapy in Acute Pain: A Systematic Review of Possible Mechanisms of Action and Clinical Effectsin Randomized Placebo-Controlled Trials," *Photomed. Laser Surg.* **24**, 158-168 (2006).
8. W. Poseteb, D. A. Wrone, D. S. Jefferey, K. A. Arndt, S. Silapunt and M. Alam, "Low-Level Laser Therapy for Wound Healing: Mechanism and Efficacy," *Dermatol. Surg.* **31**, 334-340 (2006).
9. A. S. da Rosa, A. F. dos Santos, M. M. da Silva, G. G. Facco, D. M. Perreira, A. C. A. Alves, E. C. J. Pinto Leal and P. d. T. Camillo de Carvalho, "Effects of Low-level Laser Therapy at Wavelengths of 660 and 808 nm in Experimental Model of Osteoarthritis," *Photochem. Photobiol.* **88**, 161-166 (2012).
10. J. Taradaj, A. Franek, L. Cierpka, P. Krol, E. Blaszczak, P. Dolibog and D. Kusz, "Failure of low-level laser therapy to boost healing of venous leg ulcers in surgically and conservatively treated patients," *Phlebologie* **37**, 227-282 (2008).
11. S. L. Jacques and M. Keijzer, "Dosimetry for lasers and light in dermatology: Monte Carlo simulation of 577-nm pulsed laser penetration into cutaneous vessels." in Lasers in Dermatology and Tissue Welding, O.T. Tan, R.A. White and J.V. White, Ed., *Proc. SPIE* **1422**, 2-13 (1991).
12. M. J. C. van Gemert, D. J. Smithies, W. Verkruysse, T. E. Milner and J. S. Nelson, "Wavelengths for port wine stain laser treatment: influence of vessel radius and skin anatomy." *Phys. Med. Biol.* **42**, 41-50 (1997)

13. B.Choi, B. Majaron, and J. S. Nelson. "Computational model to evaluate port wine stain depth profiling using pulsed photothermal radiometry." *J. Biomed. Opt.* **9**, 299-307, (2004)

14. W. C. Y. Lo and L. Lilge, "Acclerated 3-d Monte Carlo light dosimetry using a graphics processing unit (gpu) cluster." in Laser Applications in Life Sciences, M. Kinnunen and R. Myllyla, Ed., *Proc. SPIE* **7376**, 737609 (2010).

15. L. Wang, S. L. Jacques and L. Zheng, " MCML – Monte Carlo Modeling of light transport in multi-layered tissues." *Comput. Methods Programs Biomed.* **47**, 131-146 (1995)

16. S. Prahl, M. Keijzer, S. L. Jacques and A. J. Welch, " A Monte Carlo Model of Light Propagation in Tissue" in Dosimetry of Laser Radiation in Medicine and Biology, *Proc. SPIE* **IS 5***,* 102-111 (1989).

17. T. Roeva, T. Petrov and N. Minkovsky, "Results of the trials and light delivery evaluation at low level laser therapy of acute and chronic pain," in Eghit International Conference on Laser and Laser Information Technologies, V.Y. Panchenko and N.V. Sabotinov, Ed., *Proc. SPIE* **5449***,* 489-493 (2004).

18. E. Stoykova and O. Sabotinov, "Precise optical dosimetry in low level laser therapy of soft tissues in oral cavity," in Eghit International Conference on Laser and Laser Information Technologies, V.Y. Panchenko and N.V. Sabotinov, Ed., *Proc. SPIE* **5449***,* 474 (2004).

19. P. Parvin, S. Eftekharnoori and H. R. Dehghanpour, "Monte Carlo Simulation of Photon Densities Inside the Dermis in LLLT (Low Level Laser Therapy)," *Opt. Spectrosc.* **107**, 486-490 (2009).

20. N. Honda, T. Nanjo, K. Ishii, K. Awazu, "Optical properties measurement of laser coagulated tissues with double integrating sphere and inverse Monte Carlo technique in the wavelength range from 350 to 2100 nm," in Optical Interactions with Tissue and Cells XXII, E.D. Jansen and R.J. Thomas, Ed., *Proc. SPIE* **8221**, (2012).

21. A. N. Bashkatov, E. A. Genina and V. V. Tuchin, "Optical Properties of Skin, Subcutaneous, and Muscle Tissues: A Review," *J. Innov. Opt. Health Sci.* **4**, 9-38 (2011).

22. A. N. Bashkatov, E. A. Genina, V. I. Kochubey and V. V. Tuchin, "Optical Properties of Skin, Subcutaneous, and Muscle Tissues in the wavelength range from 400 to 2000 nm," *J. Phys. D: Appl. Phys.* **38**, 2543-2555 (2005).

23. N. Rajaram, T. H. Nguyen and J. W. Tunnell, "Lookup table-based inverse model for determining optical properties of turbid media," *J. Biomed. Opt.* **13**, (2008).

24. R. Hennessy, S. L. Lim, M. K. Markey and J. W. Tunnell, "Monte Carlo lookup table-based inverse model for extracting optical properties from tissue-simulating phantoms using diffuse reflectance spectroscopy," *J. Biomed. Opt.* **18**, (2013).

25. J. Bensouilah, P. Buck, R. Tisserand and A. Avis, *Aromadermatology: Aromatherapy in the Treatment and Care of Common Skin Conditions*, Radcliffe Publishing, Abington (2006).

26. R. Marchesini, A. Bertoni, S. Andreola, E. Melloni and A. E. Sichirollo, “Extinction and absorption coefficients and scattering phase functions of human in vitro,” Appl. Opt. 28, 2318-2324 (1989)

27. C. R. Simpson, M. Kohl, M. Essenpreis and M. Cope, “Near-infrared optical properties of ex vivo human skin and subcutaneous tissues measured using the Monte Carlo inversion technique,” Phys. Med. Biol. 43, 2465-2478 (1998).

28. M. F. Modest, *Radiative Heat Transfer*, Academic Press, New York (2003).

29. T. L. Troy and S. N. Thennadil, “Optical properties of human skin in the near infrared wavelength range of 1000 to 2200 nm,” *J. Biomed. Opt.* **6**, 167-176 (2001).

30. I. V. Meglinski and S. J. Matcher, “Quantitave assessment of skin layers absorption and skin reflectance spectra simulation in the visible and near-infrared spectral regions,” *Physiol. Meas.* **23**, 741-753 (2002).

31. C. A. Gueymard, D. Myers and K. Emery, “Proposed Reference Irradiance Spectra for Solar Energy Systems Testing,” *Sol. Energy* **73**, 443-467 (2002).

32. K. Iino, K. Maruo, H. Arimoto, K. Hyodo, T. Nakatani and Y. Yamada, “Monte Carlo Silmulation of Near Infrared Reflectance Spectroscopy in the Wavelength Range from 1000 nm to 1900 nm,” *Opt. Rev.* **10**, 600-606 (2003).

33. N. Metropolis and S. Ulam, “The Monte Carlo Method,” *JASA* **44**, 335-341 (1949).

34. H. Kahn and T.E. Harris, “Estimation of particle transmission by random sampling Monte Carlo method” *Nat. Bur. Std. Appl. Math.* **12**, 27-30 (1951).

35. D. M. Wieliczka, S. Weng and M. R. Querry, "Wedge shaped cell for highly absorbent liquids: infrared optical constants of water," *Appl. Opt.* **28**, 1714-1719 (1989).
36. H. C. van de Hulst, *Multiple Light Scattering*, Academic Press, New York (1980).
37. S. Saghafi, M. Wothford, M. Farhadi. F. Moravej, R. Ghaderi, A. Geranmayeh and Z. Ghoranneviss, "Effects of laser beam shapes on depth of penetration in dermatology" in Biophotonics and New Therapy Frontiers, R. Grzymala and O. Haeberle, Ed., *Proc. SPIE* **6191**, 619107 (2006).
38. B. Chen, R. J. Thomas, A. J. Welch, " Modeling thermal damage in skin from 2000-nm laser irradiation" *J. Biomed. Opt.* **11**, 064028 (2006).
39. C. P. Chain, G. D. Polhamus, W. P. Roach, D. J. Stolarski, K. J. Schuster, K. L. Stockton, B. A. Rockwell, B. Chen, A. J. Welch, "Porcine skin visible lesion thresholds for near-infrared lasers including modeling at two pulse durations and spot sizes" *J. Biomed. Opt.* **11**,041109 (2006).
40. American National Standards Institute, Inc, *American National Standard for Safe Use of Lasers,* Laser Institute of America, Orlando (2007).
41. A. Forsgren, P. E. Gill, M. H. Wright, "Interior Methods for Nonlinear Optimization," SIAM Rev. **44**, 525-597 (2002).
42. R. G. Giovanelli, "Reflection by Semi-infinite Diffusers," Optica. Acta.**2**, 153-162 (1955).
43. J. D. Hardy, H. T. Hammel and D. Murgatroyd, "Spectral Transmittance and Reflectance of Excised Human Skin," J. Appl. Physiol. **9**, 257-264 (1956)

Vita

Babak Nasouri received a Bachelor of Science in Mechanical Engineering from Sharif University of Technology in June 2012. His bachelor thesis was on simulating and characterizing the cycle variability of Homogeneous Charge Compression Ignition (HCCI) combustion. He began graduate study in the Thermal/Fluid Systems track of Mechanical Engineering department at The University of Texas at Austin in the fall of 2012. In January 2013, he began his research with Dr. Halil Berberoglu in the Solar Energy and Biofuels Laboratory, where his study was focused on laser propagation through participating media.

Permanent Email Address: babak.nasouri@gmail.com

This thesis was typed by the author.